Department of Chemical Engineering

Investigation of Inhibition Performance of Kinetic Hydrates Inhibitors

Shuo Wang

This thesis is presented for the Degree of
Master of Engineering (Chemical Engineering)
of
Curtin University

October 2012

Declaration

To the best of my knowledge and belief this thesis contains no materials previously published by any other person except where due acknowledgement has been made.

This thesis contains no material which has been accepted for the award of any other degree or diploma in any university.

Signature :

Date : 2nd October 2012

Abstract

The aim of this thesis is to investigate the inhibition process of tetrahydrofuran (THF) hydrates in the presence of two kinetic hydrate inhibitors (KHIs) and the effect of these KHIs on the formation and growth of THF hydrates under various experimental conditions, using a ball-stop rig and a rheometer. Two well-known KHI polymers, poly(*N*-vinylcaprolactam) (Luvicap® EG) and poly(vinylcaprolactam/ vinylpyrrolidone/ dimethylaminoethyl methacrylate) (Gaffix® VC-713) were selected for the investigation. Other chemicals, including ethanol, ethylene glycol and sodium chloride salt, were used to investigate their synergic effect upon the KHIs.

Using a ball-stop rig, the effects of salt concentration, inhibitor concentration, type of solvent and solvent concentration on inhibitor performance were investigated at a constant temperature. A new concept, *critical concentration*, was proposed for evaluation and interpretation of the inhibition performance of KHIs.

Using a rheometer, the inhibition behaviour of the two KHIs in various concentrations were investigated. Detailed information regarding hydrate formation and inhibition in the presence of the KHIs was presented and analysed based on key parameters, including environmental temperature (T_e), induction time (t_i), onset temperature (T_{onset}), maximum shear stress (τ_{max}) and time of total plugging (t_{tp}). The results demonstrate the importance of T_{onset} in relation to evaluation and application of the KHIs. They only present their superior kinetic hydrate inhibiting performance when the T_e is above the T_{onset}. As is well-known by crystallographers, when the temperature of a hydrate-forming solution is lower than its T_{onset}, hydrates form

rapidly regardless of the presence of the inhibitors. Overall, the investigation indicated that, for the ball-stop rig testing, reliable information was obtained only if the concentration of the inhibitor was above a critical concentration, below which the testing results scattered drastically and were inconsistent. Salt and solvent concentrations and other additives present in the operating systems should be considered when a suitable KHI concentration is determined for a particular field application; in rheological testing, parameters T_e, t_i, T_{onset}, τ_{max} and t_{tp} are determined to describe the inhibition process of KHIs. The results also demonstrate the importance of T_{onset} in KHI evaluation and subsequent applications.

The experimental approaches established and the information obtained from this work are valuable for gaining insight and understanding, and for developing adequate applications of kinetic hydrate inhibitors.

Acknowledgements

The completion of this research has involved much help from many people. My sincere appreciation goes to the following individuals, whose guidance and support made this work possible:

I would like to thank my thesis advisor A/Prof.Xia Lou for her guidance, support and great patience. I am so deeply grateful for the opportunity to join her research group and conduct my Master work under her supervision. Her vision and dedication to research have been truly inspirational.

I would like to thank A/Prof. Steve Errington, Prof. Ming Ang and Prof. Moses Tadé for their support and help.

I would also like to thank hydrates research group member, Dr Ailin Ding, and undergraduate students, Tina Pelemis and Carmelo Crisafio, for their assistance in some rig testing experiments.

My appreciation must also go to Dr Ailin Ding, Chao Li, Linxi Ruan, Yenny and Yuli for their friendship, which created a pleasant working environment.

Many thanks are given to those who provided great help during my research work. These include Grant Cope, Kristy Blyth, Dr Peter Sheppard, Peter Chapman and Tomoko Radomirovic (Department of Chemistry, Curtin); Naomi Tokisue, Karen Hynes, Ann Cornell and Zero Zhang (Department of Chemical Engineering, Curtin); and Kelly Clark (Office of Research and Development).

Finally, I would like to thank my wife and my parents for their love, support, encouragement and understanding.

This thesis is dedicated to my beloved family

Publications and Conference Presentations

Peer Reviewed Journal Papers

- Ding, A. L., Wang, S., Pelemis, T., Crisafio, C. and Lou, X. 2010. Specific critical concentrations of low dosage hydrate inhibitors in a THF-NaCl hydrate formation solution. Asia-Pacific Journal of Chemical Engineering 5(4): 577-584

- Lou, X., Ding, A.L., Maeda, N., Wang, S., Kozielski, K. and Hartley, P. Synthesis of Effective Kinetic Inhibitors for Natural Gas Hydrates. Energy & Fuels 2012, Vol.26(2), pp.1037-1043

Peer Reviewed Full Conference Papers

- Wang, S., Pelemis, T., Crisafio, C., Ding, A. L., and Lou, X. 2009. Evaluation of Hydrate Inhibition by Modified Ball Stop Rig and Novel Rheology System. In Proceedings of Chemeca2009.Perth, Australia, 27–30 September 2009.

- Ding, A. L., Wang, S., Pelemis, T., Crisafio, C. Kozielski, K., and Lou, X. 2009. Concentration Effect on the Inhibition Efficiency of Low Dose Hydrate Inhibitors. In Proceedings of Chemeca2009. Perth, Australia, 27–30 September 2009.

Conference Abstract

- Pelemis, T., Wang, S., Lou, X. 2012. Solvent synergy effect on kinetic hydrate inhibitors. Golden Research Conference on Natural Gas Hydrates Systems. Ventura, CA. USA. 18-29 March 2012.

Contents

List of figures

List of tables

CHAPTER 1 Introduction

1.1 Background

1.1.1 Gas hydrates

The formation of a gas hydrate was first discovered in 1811, when Sir Humphrey Davy obtained chlorine hydrate by cooling an aqueous solution of saturated chlorine gas to below 9 ^{o}C (Sloan and Koh, 2008). At that time, the study of gas hydrates attracted mere curiosity and remained as a purely academic pursuit until, in 1934, Hammerschmidt reported that gas hydrates were responsible for the blockage of flow lines, valves and wellheads. When he discovered thermodynamic inhibitors (Hammerschmidt, 1934), the study of gas hydrates started to attract more attention from both industrial and academic people.

Gas hydrates are ice-like clathrate crystalline inclusion compounds consisting of intermolecular polyhedral water cavities in which small non-polar molecules (typically gases) are trapped inside "cages" of hydrogen-bonded water molecules (Chatti et al., 2005). In other words, clathrate hydrates are clathrate compounds in which the host molecule is water and the guest molecule is typically a gas (Mahajan et al., 2007). The guest molecules are necessary to support the cavities. The bonding between host and guest molecules is principally physical attraction, rather than the stronger chemical bonding responsible for most compounds. For instance, hydrate water-ice lattice is hydrogen-bonded and, without the support of the trapped molecules, the lattice structure of hydrate clathrates would collapse into a conventional ice crystal structure or liquid

water. Most low molecular weight gases, including O_2, H_2, N_2, CO_2, CH_4, C_2H_6, Cl_2, H_2S, Ar, Kr, and Xe, form hydrates under certain conditions. Higher hydrocarbons and freons form hydrates at suitable temperatures and pressures (Sloan and Koh, 2008). Some substances that are in liquid form at room temperature also form hydrates at low temperature and atmospheric pressure. For example, tetrahydrofuran (THF) forms hydrate at 4.4 ℃ at atmospheric pressure (Koh, 2002). Other liquid molecules that form hydrates include benzene, cyclopentane, methylcyclopentane, cycloheptane, methylcyclohexane and ethylcylopentane (Pickering et al., 2001). Theoretically, gas hydrates may form in any location where a free guest molecule exists with water and both the appropriate temperature and pressure. This can be in outer space, in the atmospheres of planets, inside the planets, and/or within technical systems of production, transportation and processing of gases (Loveday et al., 2001).

1.1.2 Common structure of gas hydrates

There are three common crystal structures of gas hydrates: cubic structure I, cubic structure II and hexagonal structure H (Ripmeester et al., 1987, Long and Sloan, 1993). Among these three structures, cubic structure I is the most common form within the Earth's natural environments, and it forms with single guest molecules that are between 0.42–0.55 nanometres in diameter. Examples are methane, ethane, carbon dioxide and hydrogen sulphide. Cubic structure II occurs mostly in man-made environments. Molecules that are either smaller than 0.42 nanometres, such as nitrogen and hydrogen, or between 0.6 and 0.7 nanometres, such as propane or iso-butane, often form structure II. Hexagonal structure H may occur in both natural and artificial environments, but only forms in the presence of larger molecules that are between 0.7 and 0.9 nanometres and are accompanied by the presence of smaller molecules. Iso-pentane and 2,2-dimethylbutane

form such a structure when accompanied by methane, hydrogen sulfide or nitrogen (Sloan, 2003b, Ribeiro and Lage, 2008).

All three types of hydrate structure are built upon five basic water molecule cavities: **pentagonal dodecahedron, tetrakaidecahedron, hexakaidecahedron, irregular dodecahedron** and **icosahedron** (Figure 1.1). Guest molecules are trapped inside the cavities depending upon their sizes (Sloan, 1998a).

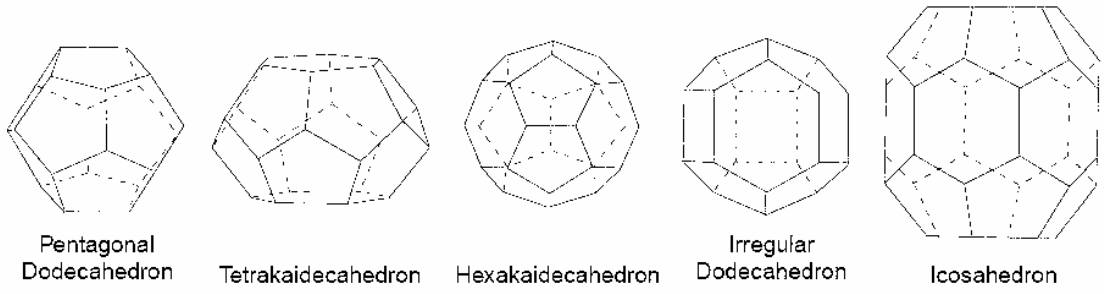

Figure 1.1 The five basic water molecule cavities of gas hydrate structures (Sloan, 1998b)

Figure 1.2 shows the unit cells of gas hydrates in cubic structure I, cubic structure II and hexagonal structure H. **Structure I** gas hydrates contain 46 water molecules per unit cell arranged in two dodecahedral cavities and six tetrakaidecahedral cavities which can accommodate, at most, eight guest molecules up to 5.8 Angstroms in diameter. Structure I allows the inclusion of both methane and ethane but not propane (Sloan, 2003a). **Structure II** gas hydrates contain 136 water molecules per unit cell arranged in 16 dodecahedral cavities and 8 hexakaidecahedral cavities, which can also accommodate up to 24 guest molecules, but to a larger diameter of 6.9 Angstroms. This allows the inclusion of propane and iso-butane in addition to methane and ethane (Sloan, 2003a). **Structure H** gas hydrates, which contain 34 water molecules per unit cell arranged in three pentagonal dodecahedral cavities, two irregular dodecahedral cavities and one icosahedral cavity, can accommodate even larger guest molecules such as iso-pentane

(Sloan, 2003a).

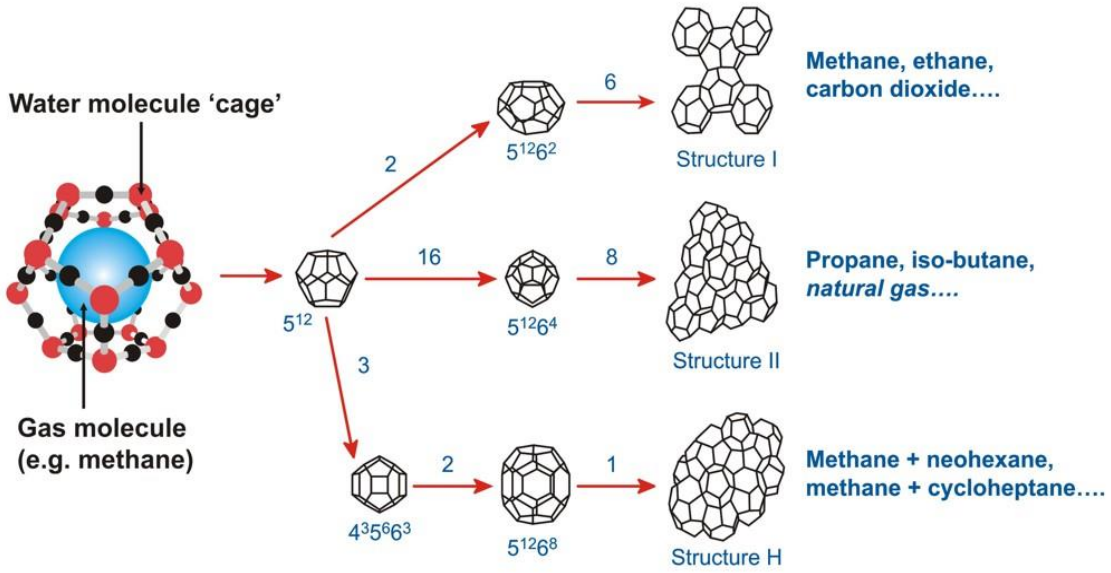

Figure 1.2 The three common hydrate crystal structures (Sloan, 2003a)

Generally, in all three structures there is only one guest molecule within each cage. However, at very high pressure, two small guests such as hydrogen and a noble gas, may occupy the same cage at one time (Sloan, 2003a). Structure I and Structure II are common hydrates which appear in common industrial procedures but structure H was more recently developed in a laboratory (Mehta and Sloan, 1996).

1.1.3 Industrial impact of gas hydrates

The formation of natural gas hydrates in gas and oil production and transmission pipelines can lead to blockage (Sloan, 1998b), which will stop production and sacrifice the structural integrity of both sub-sea pipelines and surface facilities. Figure 1.3 shows pipelines blocked by hydrates. Significant investment is required to prevent hydrate blockages in sub-sea gas and oil transmission pipelines. For example, offshore operations spend approximately a million USD per mile for insulation of subsea pipelines to prevent hydrate blockages (Lederhos et al., 1996). The unexpected blockage of a flow channel can

lead to significant economic loss and ecological risks, as well as potential safety hazards (Urdahl et al., 1995a) to exploration and transmission personnel. Therefore, prevention of hydrate blockages within flow channels has been a critical issue and significant effort has been made by the oil and gas industry to keep pipelines free of hydrates blockages. Gas hydrate inhibition has become a high demand research area (Lederhos et al., 1996, Kelland, 2006).

Figure 1.3 Hydrate blockage in pipeline (Alapati and Davis, 2007)

On the other hand, natural gas hydrates are very promising mineral energy resources. Gas stored in a hydrate state has been reported as a most efficient, convenient and economical gas storage method at relatively low pressures (Kerr, 2004, Chatti et al., 2005, Sloan and Koh, 2008). Experts have estimated the potential total deposit of natural gas in hydrate state on Earth to be 15×10^{15} m^3, which is higher than the surveyed world resources of hydrocarbon gases by two orders of magnitude (Englezos, 1993). Therefore, natural gas hydrates will be a very important energy resource for the world in future decades (Kvenvolden, 1988, Englezos and Lee, 2005, Dawe and Thomas, 2007, Makogon et al., 2007, Moridis et al., 2011). Figure 1.4 is a picture of world occurrences of known gas hydrate accumulations.

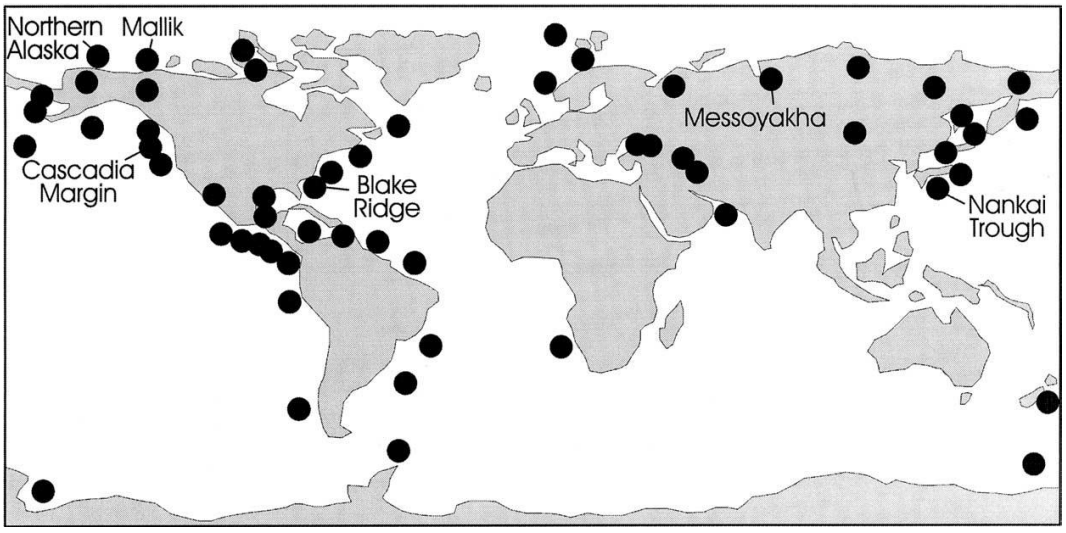

Figure 1.4 World occurrences of known gas hydrate accumulations (Beauchamp, 2004)

In addition, there are many other applications of hydrate technology. For instance, hydrate technology can be used to remove/purify water from an aqueous solution when a hydrate-forming fluid is in contact with an aqueous solution at a temperature at which hydrate can form. The hydrate-forming fluid and at least part of the water constituent of the solid hydrate are separated from the solute to produce a substantially hydrate-forming fluid-free product comprising the solute and any remaining water (Englezos, 1993, Purwanto et al., 2001, Chatti et al., 2005). Hydrate technology also has been applied in the refrigeration process. The hydrate slurries can be used as two phase refrigerants (Fournaison et al., 2004, Xie et al., 2005, Ogawa et al., 2006). Gas hydrates also have been used for dissipation of fogs (Makogon, 1997, Sloan and Koh, 2008), small scale cold storage applications (Xie et al., 2010) and flame retardancy (Liu et al., 2011, Cong et al., 2011). This work will only focus on the inhibition of hydrates.

1.1.4 Gas hydrate inhibition

Various strategies have been investigated in order to prevent hydrate formation and to ensure regular flow in oil and gas operations. These include mechanical, thermal, hydraulic and chemical methods (Chatti et al., 2005).

The mechanical method involves monitoring pressure distribution at critical sections of a pipeline to diagnose hydrate accumulation levels (Chatti et al., 2005). Then, pistons or gaseous plugs can be used throughout the pipeline to remove accumulated hydrates in order to prevent serious hydrate plugs (Yu and Cheng, 2009, Chatti et al., 2005).

The thermal method involves built-in insulation structures within a pipeline and a local heat flow delivery system that keeps the fluid product temperature above the hydrate-forming temperature to minimize the thermodynamic possibility of hydrate formation (Kelland et al., 2000, Chatti et al., 2005, Halvorsen et al., 2000).

The hydraulic method is used to minimize water content in the mass transportation process. Hydraulic control fluids can be used to almost completely remove water within product flow in order to prevent hydrates from forming (Knepper et al., 2009).

These mechanical, thermal and hydraulic hydrate plug prevention methods can be a good choice in certain situations. In some cases, these methods have to be used together with chemical injection for flow assurance of oil and gas pipelines.

The chemical method, which is most commonly used for gas hydrates blockage prevention, is to inject a high concentration (40 vol% to 60 vol%) of 'Thermodynamic'

inhibitors, such as alcohols (Ng and Robinson, 1985, Bobev and Tait, 2004), glycols (Wang et al., 2003, Yousif, 1998), aqueous electrolytes, or a combination of these and others, into a pipeline (Dholabhai et al., 1993, Chun et al., 2000). These inhibitors act to decrease the onset temperature of the hydrates' crystallite formation by increasing the critical energy requirement of thermodynamic equilibrium of both the water and gas phases (Makogon et al., 2000), in a similar way that a coolant decreases the freezing point of water. Methanol and glycols (Mokhatab et al., 2007) are the most widely applied hydrate inhibitors used by the oil and gas industry. Although these methods have proven to be effective in preventing gas hydrate formation, the usage of glycol or methanol is usually associated with high operating capital costs (Sloan and Fleyfel, 1992). Large volumes of the inhibitors are required (Sloan et al., 1998, Wu and Englezos, 2006) and the cost associated with the operation and recovery of the inhibitors is very high. The environmental impact is also a concern due to the high amounts of thermodynamic inhibitors required to control hydrates. Worldwide annual expenses for methanol alone were estimated at US$220 million in 2003 (Sloan, 2003b).

Driven by the need to cut operating costs and reduce the environmental impact of operating oil and gas facilities, many recent research and development activities have concentrated on the design and development of novel, cheap and environmentally friendly low-dosage hydrate inhibitors (LDHIs) (Kelland, 2006, Del Villano et al., 2008). Over the last two decades, hydrate research has focussed more on kinetic studies to discover an alternative technology to control hydrate formation within pipelines by using LDHIs (Lederhos et al., 1996). LDHIs are new types of chemicals that are able to prevent the nucleation and/or growth of gas hydrates with an effective dosage typically less than 1 wt% in the aqueous phase (Sloan et al., 1998, Kelland, 2006). This is much lower than that

required for thermodynamic inhibitors. Unlike thermodynamic inhibitors that shift the thermodynamic equilibrium of hydrates, LDHIs either delay hydrate formation so that the time required for the hydrate to form is longer than the residence time of the gas in the pipeline, or allow hydrate formation but prevent the agglomeration of formed hydrate crystals so that the total plugging of pipelines is prevented (Yousif et al., 1994, Lederhos et al., 1996, Kelland et al., 2008). Therefore, those hydrate inhibitors are also called time-dependent inhibitors. Clearly, a suitable cost-effective low-dosage inhibitor will produce significant improvements in controlling hydrate formation, both economically and ecologically (Kelland, 2006).

LDHIs have been divided into two basic categories: kinetic hydrate inhibitors (KHIs) and anti-agglomerants (AAs) (Del Villano et al., 2008, Kelland, 2006). Chemicals that delay hydrate formation are classified as KHIs. Primarily KHIs act as gas hydrate anti-nucleators, and most of them also retard the growth of gas hydrate crystals. KHIs do not completely prevent hydrate formation and growth. Actually, the kinetic hydrate inhibition system allows hydrates to form, but with a delay in time, and it also retards the growth of the hydrates (Sloan et al., 1998, Del Villano et al., 2008). KHIs allow you to transport hydrate-forming fluids, for a certain period of time, before chunky hydrate crystals start to form. The time at which the first hydrate crystals form is called the induction time (Lederhos et al., 1996).

KHIs are usually water soluble polymer-based chemicals. Some examples of known and patented KHIs are poly(N-vinylpyrrolidone) (PVP), poly(N-vinylcaprolactam) (PVCap), poly(N-methyl-N-vinylacetamide) (VIMA), polyethylacrylamide (PEAA) and their copolymers or blends. Figure 1.5 displays the chemical structure of three kinetic

inhibitors, poly(vinylcaprolactam/ vinylpyrrolidone/ dimethylaminoethyl methacrylate) (Gaffix®VC-713), polyvinylcaprolactam (PVCap) and poly(vinylpyrrolidone)(PVP) that are commonly used as standards for performance comparisons of KHIs. There also are a number of non-polymeric hydrate crystal growth inhibitors such as tetrapentylammonium bromide and butoxyethanol. These chemicals often work as KHI synergists (Lederhos et al., 1996, Freer and Sloan, 2000, Kelland, 2006).

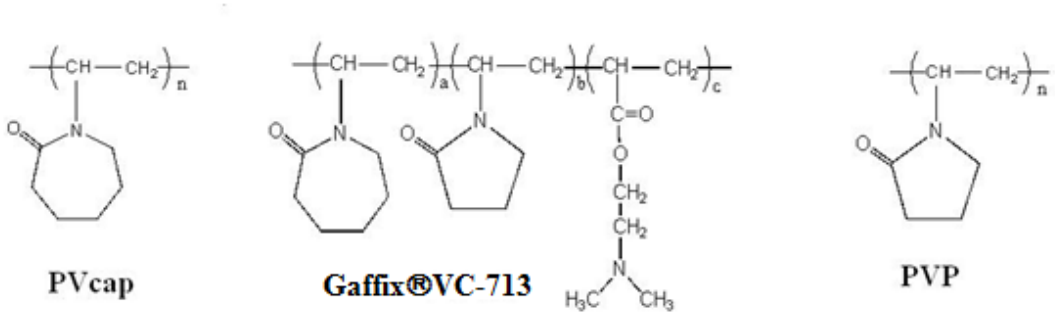

Figure 1.5 Chemical structure of three common KHIs (PVcap, Gaffix®VC-713 and PVP)

AAs prevent hydrates from growing into big blockages by preventing agglomerations of hydrate crystals. They allow hydrates to form, but they prevent them from agglomerating and subsequently accumulating into large masses (Gaillard et al., 1999, Kelland et al., 2008). An AA enables the hydrates to form as transportable non-sticky slurry of hydrate particles dispersed in the liquid hydrocarbon phase. AAs are generally surface active chemicals that prevent both the growth and the agglomeration of hydrate crystals (Huo et al., 2001, Kelland et al., 2009). Typical AAs reported are quaternary ammoniums and phosphoniums (Figure 1.6) (Kelland, 2006).

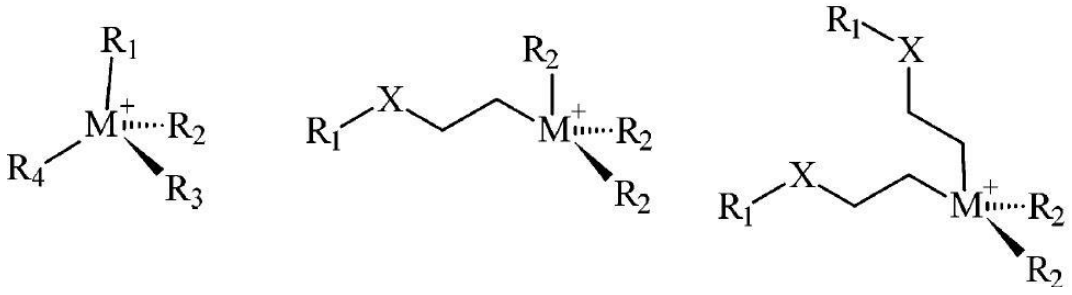

Figure 1.6 Structure of quaternary ammonium orphosphonium as hydrate growth inhibitors

(Note: M = N or P, and R groups are n-butyl, n-pentyl or isopentyl; X represents an optional spacer group.)

So far, both kinetic inhibitors (KHIs) and anti-agglomerants (AAs) have been tested in field applications by large oil companies. Up until 2005, there have been 50-70 field applications of low-dose hydrate inhibitors (LDHIs), the majority of which are related to KHIs. Currently, hydrate inhibitor research extends to exploiting the synergistic blending inhibition system to obtain better low-dose hydrate inhibitors (Heidaryan et al., 2010). Blends of thermodynamic inhibitors and KHIs also have been tested in the field. Although some have shown promise in hydrate inhibition, the extensive application of such inhibitors currently is limited, partly due to the unsatisfactory inhibition efficiency (Kelland, 2006).

1.1.5 Research activities on KHIs

KHIs are generally economical and eco-friendly. However, hydrates may still form and block the pipeline due to the time-dependent nature of KHIs, especially when the transportation time of natural gas through the pipeline is too long (Pickering 2001). Therefore, many researchers have put effort into improving the performance of KHIs. The

research works can been divided into three areas - synergism of KHIs, development of new KHIs and mechanism studies.

Synergism is a method of introducing one or more additives into the inhibition system in order to enhance the inhibition performance of KHIs. Those additives normally are alcohols, glycols, surfactants, electrolytes and other KHIs (Dholabhai et al., 1997, Bishnoi and Dholabhai, 1999, Yousif and Young, 1994, Heidaryan et al., 2010). For example, the synergistic effect of methanol to poly(vinyl methylether), as a KHI, was discovered (Heidaryan et al., 2010). At a certain ratio of methanol to the inhibitor, a high performance synergistic hydrate inhibition system was tested for a real natural gas under gas hydrate formation conditions. Results showed that the addition of 2 wt% methanol to 0.2 wt% poly(vinyl methylether) enhanced the inhibiting efficiency of poly(vinyl methylether) by up to 10 % (Heidaryan et al., 2010). Lou et al (2010 and 2012) also reported the synergistic effects of both ethanol and ethylene glycol upon the inhibition behaviour of Gaffix® VC-713, Luvicap® EG and a series of newly developed KHIs. Cationic tetraalkylammonium ions (particularly for alkyl = butyl or pentyl) have been used as synergists for commercial kinetic hydrate inhibitor polymers (KHIs), such as N-vinylcaprolactam polymers (Sefidroodi et al., 2011). More recently, the hydrate inhibition performance of imidazolium-based ionic liquids was investigated. The report showed that the imidazolium-based ionic liquids clearly acted as synergists for the hyperbranched poly(ester amide)-based KHI (Del Villano and Kelland, 2011). Also, trialkylamine oxide was reported as a synergist to enhance the performance of polyvinylcaprolactam (PVCap) (Kelland et al., 2012).

Development of novel KHIs has not stopped. One example is polyaspartamides that are

made from polysuccinimide and are biodegradable. However, polyaspartamides are not very compatible with commercial KHI polymers (Chua et al., 2011). A series of copolymers made of polyethylene glycol, *N*-vinylcaprolactam (PEO-co-VCap), tetrahydrofurfuryl methacrylate and methyl methacrylate have been developed by our own group. Studies on these new KHIs have shown that they are as effective as Luvicap® EG and Gaffix® VC-713, in preventing the formation of THF hydrate (Lou et al., 2012). In preventing formation of natural gas hydrates, these new KHIs are more effective than Luvicap® EG and Gaffix® VC-713. Poly(N-vinyl piperidone) (PVPip) is another KHI that has been developed recently. It was reported that PVPip with a molecular weight of 4,000 performed better as a KHI than PVP but worse than PVCap, both being of similar molecular weights (O'reilly et al., 2011).

Some recent research works have focused on mechanism studies and molecular-dynamics simulations. A molecular-dynamics simulation of hydrate inhibition was established by Davenport et al. in 2011. The interaction of OH---O and CH---O hydrogen bonding was introduced to explain the inhibition performance of KHIs at a molecular level (Davenport et al., 2011). Molecular-level understandings of the hydrate inhibition process, together with molecular-dynamics simulation, are contributing considerably to efforts in identifying and designing new KHI inhibition systems. (Hawtin and Rodger, 2006, Anderson et al., 2006)

1.1.6 Evaluation of KHIs' performances

Various reactors and equipment can be used to evaluate the performance of KHIs. These include ball-stop rig (Lederhos et al., 1996), autoclave (Del Villano and Kelland, 2011), mini-loop (Talaghat et al., 2009), loop–wheels (Urdahl et al., 1995b), rheometer (Fidel-

Dufour et al., 2006, Rensing et al., 2011), and differential scanning calorimetry (DSC) (Lachance et al., 2009). Actually, these reactors are used to provide hydrate-forming conditions, and to simulate hydrate-forming flow, using mechanical means such as bubbling, shaking or agitating, so as to mix the guest molecules with the water phase. Using these apparatus, researchers can create an hydrate-forming environment in which to evaluate the performance of KHIs at known volume, pressure and temperature.

Among these reactors, the ball-stop rig is most conveniently used for fast screening of KHIs. It was used successfully in screening over 1,500 commercially available chemicals-concentration combinations by Long et al in 1994 (Lederhos et al., 1996). The aforementioned PVP, PVCap and Gaffix® VC-713 were recognized using this method (Lederhos et al., 1996, Kelland, 2006).

A ball-stop rig is a rotating racket which controls a set of test tubes, each containing hydrate-forming solutions and a metal ball that rocks back and forth. The time of appearance of the first hydrate crystal is considered as the induction time of the tested hydrate inhibitor. When the hydrate forms and plugs the test tube, the metal ball stops moving, and this is called the ball-stop time. Induction time and ball-stop time are used as measures of the inhibition performance of the KHIs. A ball-stop rig provides a simple and effective way to quickly evaluate the inhibition efficiency of inhibitors by examining the induction time and full crystal formation time.

Rheological methods, on the other hand, have been used mostly for investigating the flow properties of clathrate hydrate slurries or hydrate-forming fluids. Rheological properties such as viscosity, yield stress and temperature can be measured readily to study the phase

change processes of hydrate slurries and hydrate-forming fluids (Delahaye et al., 2011, Peixinho et al., 2010, Fidel-Dufour et al., 2006). Rheology has been shown to be an effective and informational tool with which to analyse clathrate hydrate formation and aggregation. It also provides a novel way to detect clathrate hydrate dissociation (Rensing et al., 2008).

In many of these evaluation studies, tetrahydrofuran (THF) hydrate has been used to simulate natural gas hydrates because it forms sII hydrate, the same structure formed by natural gas, at ambient conditions of 4.4 ℃ and atmospheric pressure, at the molar ratio of 1:17 THF to water. This makes THF particularly interesting to many researchers as it can be used as an analogue to study the natural gas hydrates (Makogon et al., 1997). In addition, THF is liquid under atmospheric pressure and completely miscible with water. It is convenient to prepare the THF-Water solution at the required ratio and to minimize the variable of phase separation. There is no requirement for high pressures and complicated apparatus. THF hydrate growth can be inhibited by the same KHIs known to be effective against gas hydrates, and the testing results are generally comparable in most situations (Zeng et al., 2006).

In fact, THF hydrates have been employed in many studies to compare the inhibition efficiencies of various chemicals, including KHIs (Lederhos et al., 1996, Sefidroodi et al., 2011, Zeng et al., 2006).

1.2 Aims and methodology of the project

This project aims to study and to understand the inhibition performance of two commercially available KHIs, poly(*N*-vinylcaprolactam) (Luvicap® EG) and Gaffix® VC-713, under various experimental conditions, using a ball-stop rig and a rheometer. THF will be used as the hydrate-forming molecule. The effect of salt concentration, inhibitor concentration, solvent type and solvent concentration on inhibition performance will be investigated.

The objectives of the thesis include:

(a) Developing a practical rig and rheological method to evaluate the inhibition performance of Luvicap® EG and Gaffix® VC-713;

(b) At a selected constant temperature, measuring the ball-stop times of the THF hydrate-forming solutions in the presence of the KHIs, so as to compare their inhibition effectiveness;

(c) Investigating the effect of salt concentration and inhibitor concentration, as well as the solvent synergy effect, on ball-stop times;

(d) Investigating the inhibition performance of the selected KHIs at changing environmental temperatures, and the effect of the inhibitor concentration on their performance, using a rheometer.

The findings from this work will provide valuable knowledge that can be used to optimize the performance of the selected KHIs. The information also will be useful in designing

and developing new KHIs. The methods established in this work will be utilized to investigate other KHIs.

CHAPTER 2 Investigation of Luvicap® EG and Gaffix® VC-713 using a ball-stop rig

2.1 Introduction

Evaluation of the inhibition performance of KHIs and investigation of working conditions for KHIs during the hydrate formation process have become an important focus for the gas hydrate research community. A good measurement of KHI performance and good interpretation of experimental data could provide an effective and accurate evaluation of KHIs. This would assist in the design of new inhibitors and the creation of new technologies for effective applications of gas hydrate technologies in other industries.

In this chapter, THF hydrate-forming solutions (THF : water = 1:3 v/v) were prepared and tested using a ball-stop rig. The solutions contained either Gaffix® VC-713 or Luvicap® EG of various concentrations. Various concentrations of sodium chloride were used to mimic the ionic strength of ocean water. Varying concentrations of ethanol and ethylene glycol also were used to investigate the solvent synergy effect on inhibition performance. It should be noted that ethanol and ethylene glycol are solvents used in the commercial product of Gaffix® VC-713 and Luvicap® EG.

Shown in Figure 2.1 is a schematic design of the ball-stop rig. It was originally designed by Sloan's research group (Lederhos et al., 1996). It was used to screen over 1,500 chemicals in a THF hydrate-forming system, containing a mixture of THF and water at 1:3 v/v ratio (approximately 1:13 in molar ratio) (Long et al., 1994, Lederhos et al., 1996). The rig was further modified by many other research groups to meet the testing requirements of other hydrates systems (Arjmandi et al., 2003, Lachance et al., 2009).

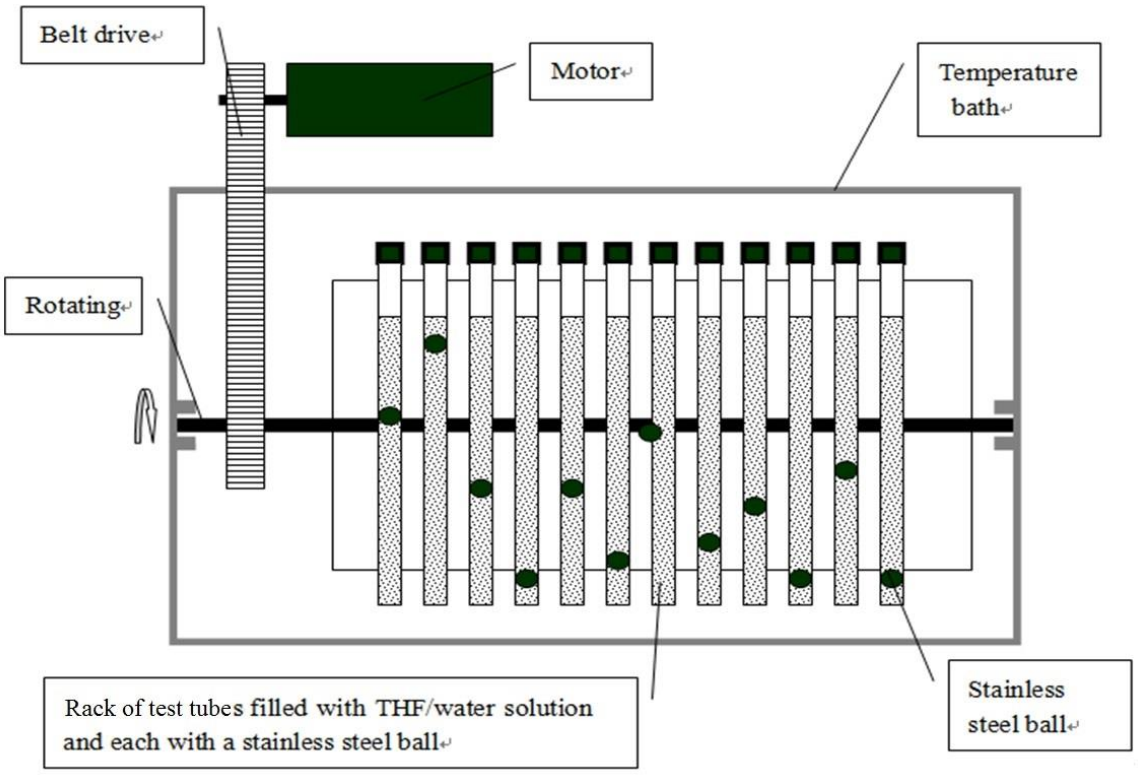

Figure 2.1 Schematic diagram of THF hydrate ball-stop rig

For operational purposes, a testing solution is injected into test tubes which contain a stainless steel ball. The test tubes are fixed on a bracket and immersed into a cooling bath (normally an ice-water mixture) and the bracket is rotated continuously by an electronic motor. The test tubes rock back and forth. When the hydrate completely plugs the test tube, the metal ball stops moving. The time is recorded as ball-stop time. Sometimes visible crystals in the test tubes were observed before the ball stopped. This was recorded as induction time. The rig used for this work will be described in more detail in the experimental section.

2.2 Experimental

2.2.1 Chemicals

Luvicap® EG, poly(*N*-vinylcaprolactam) (40 % PVCap in ethylene glycol) from BASF (Germany) and Gaffix® VC-713, poly(vinylcaprolactam/ vinylpyrrolidone/ dimethylaminoethyl methacrylate) (37 % in ethanol) were kindly donated by International Specialty Products (ISP, Germany). The chemical structures of both chemicals are displayed in Figure 1.5. Sodium chloride (Lab-Scan Analytical Science, 99 %) and deionised water were utilized in the preparation of sodium chloride solutions. Tetrahydrofuran (99 %) was purchased from Sigma-Aldrich. Ethanol (Scharlau Chemie, 99 %) and ethylene glycol (Merck, 99.5 %) were used, as purchased, without further purification.

Ethanol-free Gaffix® VC-713 was made by drying Gaffix® VC-713 (37 % in ethanol) in an oven at 70 ℃ for 48 hours.

2.2.2 Test solution preparation

1) Sodium chloride stock solution: 35 g of NaCl was weighed out and dissolved in 1,000 g deionised water to obtain one litre of NaCl 3.5 wt% stock solution (for different NaCl concentrations, the weight of NaCl was calculated correspondingly). The solution was stirred for 24 hours prior to the commencement of placement in the rig.

The 3.5 % NaCl concentration was selected to mimic the salinity of seawater (i.e., 3.5 %) according to the international standard of the American Society for Testing Materials (ASTM) D1141-98.

2) Test solutions: An accurate mass of the test inhibitor, (and, in some solutions, solvent as well), was weighed out and dissolved in a measured mass of sodium chloride solution (31.05 g, 3.5 wt%). The percentage of inhibitor weighed out was based on the total mass of deionised water and THF. This solution was magnetically stirred for approximately twenty minutes, and then THF (8.89 g) was added. This was stirred for an additional ten minutes and then visually checked to ensure that all the inhibitor had dissolved. The solution was then injected into sealed test tubes. A stainless steel ball was placed in each test tube, which was then sealed using a rubber stopper through which the solution was injected. For each solution prepared (40 mL), three test tubes were filled. Prior to the injection of each new solution, the syringe was rinsed with deionised water. It was then filled twice with the given solution and emptied back into an adequate disposal container. Containers bearing THF solutions were purged with copious amounts of tap water, then washed with detergent and deionised water, and stored in an oven (37 ℃). The same procedure was followed for the cleaning of all equipment, following the test.

3) Selection of a balance: An analytical balance, with the error bounds of +/-0.0001 g, was used for the weighing of small quantities of chemicals, including the inhibitors, ethanol and ethylene glycol. A balance, with the error bounds of +/-0.01 g, was used for the mass measurement of other materials, including the NaCl solutions and THF.

Several series of test solutions were prepared with varying concentrations of KHIs, solvents and sodium chloride. A total of 189 hydrate-forming solutions were prepared for this study. The chemical compositions of all test solutions are summarised in Table 2.1

Table 2.1 Concentrations of KHIs, NaCl and solvents in test sample solutions

Solutions	NaCl (wt%)	KHIs (wt%)		Solvents (wt%)	
		Luvicap® EG	Gaffix® VC-713	Ethanol	Ethylene glycol
NaCl effect	0, 1.0, 1.5, 2.0, 2.5, 3.0, 3.5	0.25, 0.50			0
KHI effect	3.5	0.05, 0.10, 0.15, 0.20, 0.25, 0.35, 0.50			0
Solvent effect	3.5	0	0.075	0.30	0
	3.5	0	0.15	0, 0.22, 0.30, 0.60	0
	3.5	0	0.20	0, 0.05, 0.15, 0.22, 0.30	0
	3.5	0.075	0	0	0.11, 0.20, 0.30, 0.40, 0.60, 0.80
	3.5	0.10	0	0	0.15, 0.30, 0.40, 0.60
	3.5	0.15	0	0	0.225, 0.30, 0.60

2.2.3 Ball-stop rig setup

Figure 2.2 shows the ball-stop rig and the setup for the testing. The bracket is capable of holding 12 test tubes (10mm (diameter) × 100mm (length)).The water bath dimensions are length = 600mm, width = 500mm and depth = 500mm. The water bath is covered with bubble wrap for insulation.

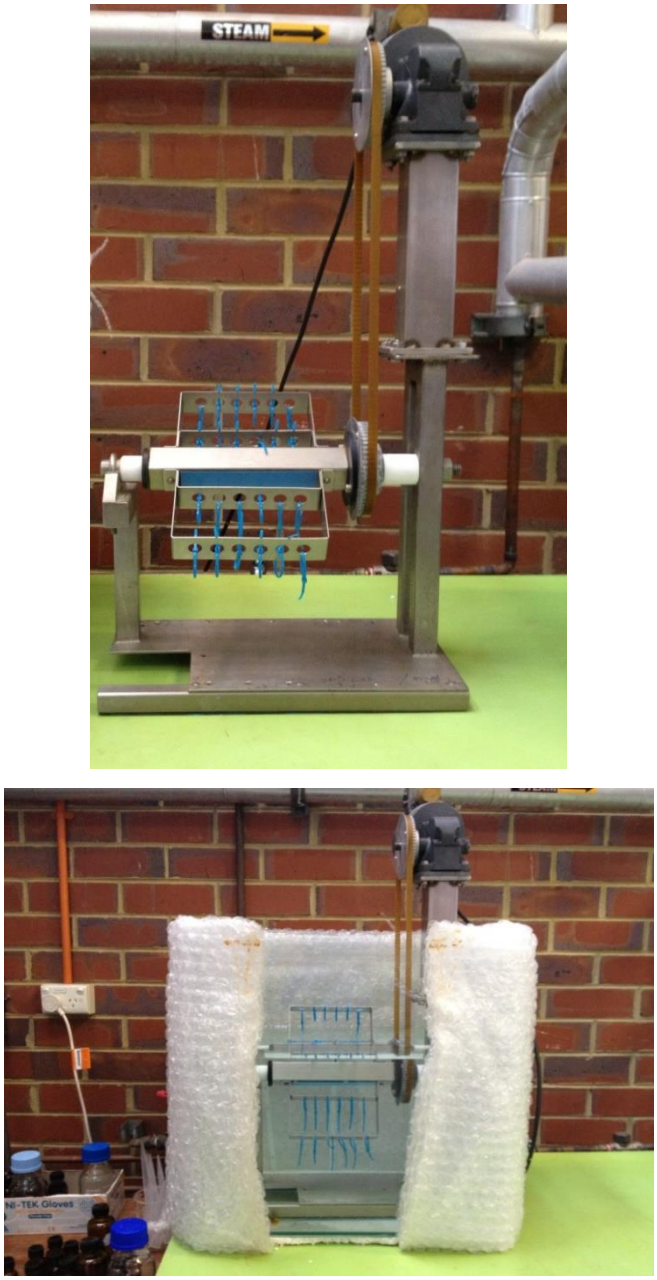

Figure 2.2 Ball-stop rig (top) and rig testing setup with a water bath (bottom)

Water Bath Preparation: The insulated glass bath was filled with ice (one-third) and water (two-thirds), and stirred, before the test solution was prepared. Every half hour, over a duration of about two hours, the solution was stirred so that the bath could reach the experimental temperature of 0 ℃ before the experiment commenced.

2.2.4 Rig testing

The prepared test tubes were mounted on the rotating rack and fastened using thin elastic bands. The entire rig was placed into the water bath at 0 ℃. After performing visual checks to ensure there were no restrictions to the rotation of the rack, the rig was turned on and the timer started. The time at which the stainless steel ball stopped moving was noted for all measurements. The testing was forcefully stopped after six hours, even if the ball was still moving. Therefore, whenever 360 minutes is quoted as the ball-stop time, it indicates that hydrate plugging had not occurred within the six hours, and this demonstrates a good inhibitor. During the rig test, the temperature was monitored at regular intervals (about every hour) to ensure it remained at 0 ℃.

All testing was carried out in triplicate.

2.3 Results and discussion

Several series of THF-NaCl solutions, varying in salt concentrations, solvent concentrations and inhibitor concentrations, were prepared and tested using the ball-stop rig. Normally, two types of data can be obtained from the rig testing. One is the hydrate induction time, representing the end of nucleation, which is indicated when hydrates or cloudy points are visually observed. The other is the time at which the ball is no longer able to move freely along the test tube due to hydrate plugging, which is recorded as ball-stop time. In our experiments, we found that the observations of the appearance of hydrate crystals or the change of cloudy points were subjective and observer-dependent. Therefore, only ball-stop time was selected as the indication of hydrate inhibition efficiency for a KHI. We also found that the values of ball-stop time were not indicative unless statistical analysis demonstrated that the differences among values from the same testing solutions were insignificant. That is to say, taking the average value of the ball-stop times for the same test solution may provide false information. Therefore, the values of ball-stop time from all test tubes, including those filled with the same test solutions, have been included in the Figures. It is known that both Luvicap® EG and Gaffix® VC-713 are very good KHIs in terms of their capacity to delay hydrate formation. At adequate concentrations, they may achieve ball-stop times greater than 24 hours. For the convenience of the study, we monitored the rig for up to 6 hours for each measurement. When the ball-stop time was greater than 6 hours, “360 min” was displayed in the results.

2.3.1 Effect of inhibitors and inhibitor concentrations on inhibition performance

As discussed in the previous section, KHIs contribute to inhibition performance. In order to investigate the effect of KHI concentration on inhibition performance alone, 3.5 wt% NaCl was used for studies of KHI concentration effects.

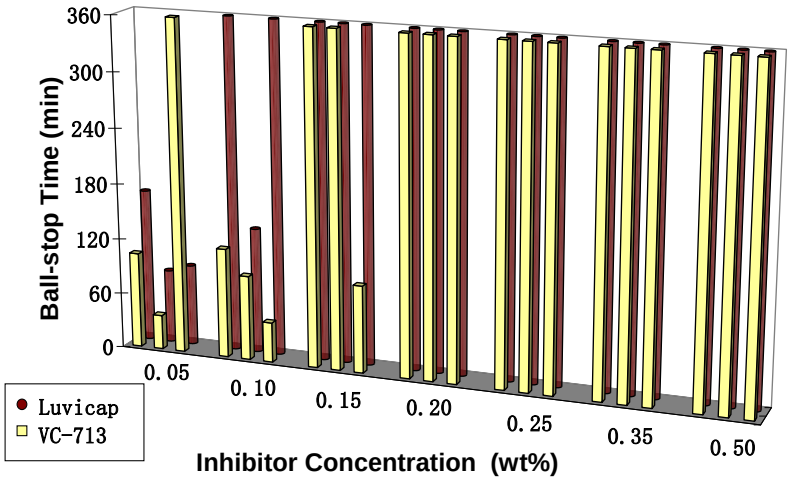

Figure 2.3 Ball-stop times for Luvicap® EG and Gaffix® VC-713 at different inhibitor concentrations in 3.5 wt% NaCl solution

Figure 2.3 shows the ball-stop time of THF-NaCl (3.5 %) solutions containing various concentrations of Luvicap® EG and Gaffix® VC-713. For Luvicap® EG, all solutions containing equal to or more than 0.15 wt% of inhibitor showed a ball-stop time greater than 360 min. When below this concentration, the results were random and could not be repeated. For Gaffix® VC-713, a similar concentration, 0.20 wt%, was found to be *critical*. At or above this concentration, the ball-stop times of three solutions were consistent and were over 360 min.

Below this concentration, the ball-stop times were inconsistent and not reproducible, even for the same test solution.

We name this concentration *specific critical concentration* (SCC). From the data displayed in the above figures, one can see also that the ball-stop time is hardly repeatable or consistent for a solution containing a KHI at less than its SCC. Therefore, comparing these values to determine the inhibition performance of LDHIs is meaningless. Knowing the SCC of a particular KHI also is important for its field applications. As the operational conditions, such as the salinity, may change in various fields, sufficient KHIs must be used to ensure adequate inhibition time for the operation.

A separate study, by our group, on the surface activities of Luvicap® EG and Gaffix® VC-713 at the air-liquid (3.5 wt% sodium chloride solution) interface has shown similar 'critical concentration' values for both the KHIs, at which the concentration dependence of the surface tension of the measured solutions changed dramatically (Rojas et al., 2010). We believe there is a strong connection between the adsorption activities and the inhibition performance of the inhibitors. Still under investigation is whether the observation of a similar critical concentration for the same KHIs in these two separate studies is a coincidence or is indicative of an intrinsic connection between the molecular interactions and the inhibition mechanisms.

It is worth mentioning that the rig testing for 0.15 and 0.2 wt% Luvicap® EG solutions was extended to 12 hours (720 min). No ball-stop time was observed. Similar observations were reported by Long et al.(1994). In their work, samples that did not show a ball-stop time within 6 hours showed no ball-stop time within 24 hours.

2.3.2 Effect of salt concentrations on inhibition performance

From our experimental data, we found that salt concentration played an important role in KHI inhibition performance. The effect of NaCl concentrations on ball-stop time for various solutions is shown in Figures 2.4 and 2.5. At the same concentration of an inhibitor, the higher the concentration of sodium chloride, the longer is the ball-stop time. This demonstrated a positive correlation between inhibition efficiency and sodium chloride concentration, which agrees well with the fact that electrolytes like sodium chloride can act as a thermodynamic inhibitor (Jager et al., 2005, Wu et al., 2007).

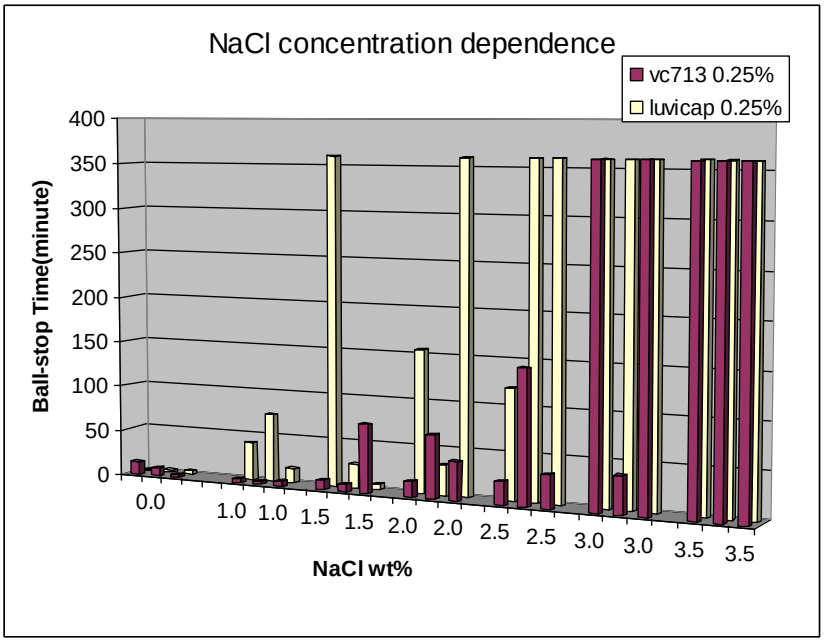

Figure 2.4 Ball-stop times for Luvicap® EG and Gaffix® VC-713 in 0.25 wt% at different sodium chloride concentrations

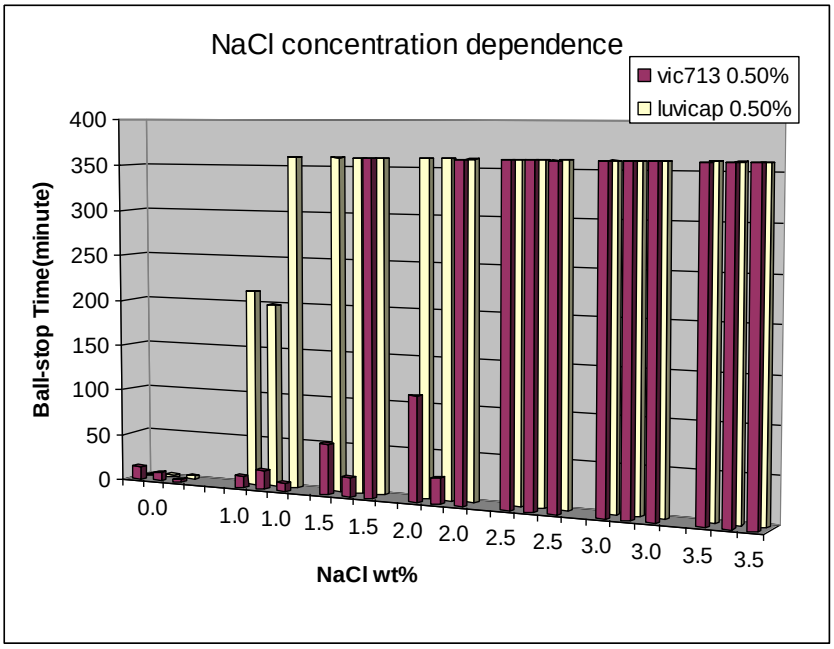

Figure 2.5 Ball-stop times for Luvicap® EG and Gaffix® VC-713 in 0.50 wt% at different sodium chloride concentrations

When comparing the data in Figure 2.4 with those in Figure 2.5, a synergistic effect is apparent. For instance, 2.5 % NaCl was required to achieve a ball-stop time consistently greater than 360 min when there was 0.5 % Gaffix® VC-713 present in the THF hydrate mixture, while at least 3.5 % NaCl was required to achieve the same ball-stop time when the mixture contained only 0.25 % Gaffix® VC-713. Similarly for Luvicap® EG, only 1.5 % NaCl was required to achieve a greater than 360 min ball-stop time when the hydrates mixture contained 0.5 wt% inhibitors. However, 3.0 wt% NaCl was required for the same ball-stop time when there was only 0.25 wt% inhibitor in the mixture. This also demonstrates that Luvicap® EG performed better than Gaffix® VC-713 in the selected concentration range (0.25 - 0.5 wt%). As can be seen in Figures 2.4 and 2.5, at 0.25 wt% of KHI, the minimum NaCl concentration required to reach a more repeatable ball-stop time (>360 min) was 3 wt% for Luvicap® EG and 3.5 wt% for Gaffix® VC-713. When the KHI concentration was increased to 0.5 wt%, the minimum NaCl concentration required to repeatedly reach a ball-stop time of 360 min was 1.5 wt% for Luvicap® EG and 2.5 wt% for Gaffix® VC-713.

Luvicap® EG is composed of 60 wt% ethylene glycol and 40 wt% PVCap containing seven-membered lactam rings attached to the polymer backbone. Gaffix® VC-713 is a terpolymer in 63 wt% ethanol. It is made of three monomer units including the VCap and a five-member ring of similar structure (Figure 1.6). These two kinetic inhibitors are thought to adsorb onto the surface of hydrate

activities during the nucleation and growth of hydrate, since the sizes of the five- and seven-member lactam rings are similar to the five- and six-member faces, respectively, in the hydrate cages. It is generally believed that the lactam rings adhere onto the hydrate crystals through hydrogen bonding with the amide groups and, hence, sterically block the further growth of hydrates. Previous literature has demonstrated that the seven-member lactam group has the most important role in the inhibiting species (Lederhos et al., 1996). Gaffix® VC-713 is a random copolymer consisting of three components. We can see from their chemical structures (Figure 1.5) that Gaffix® VC-713 contains less seven-member lactam groups than Luvicap® EG. This might be the reason that Luvicap® EG performed better than Gaffix® VC-713 at the investigated sodium chloride concentrations.

It is interesting to note that the balls stopped within minutes when no NaCl was present in the solution, no matter which KHI and what concentration was used. It seemed that, at a concentration of up to 0.50 wt%, neither Luvicap® EG nor Gaffix® VC-713 could significantly delay the hydrate formation without the presence of NaCl. This observation agrees with the results reported by Lederhos et al (1996) who examined the effect of sea salt on the inhibition efficiency of the same inhibitors using a high pressure apparatus and a natural gas mixture. The performance of the inhibitors was evaluated by the amount of gas consumed due to hydrate formation. Their experiment demonstrated that for both Gaffix® VC-713 and PVCap, at 6.89 MPa and 277.2 K, the inhibition performance deteriorated

as the sea salt concentration decreased from 3.5 wt% to 0 wt%. More inhibitors were required to ensure effective prevention of gas hydrate formation when salt was not present in the system. It is not surprising to find that, in our investigated KHI concentration range (0.25 to 0.50 wt%), neither Luvicap® EG nor Gaffix® VC-713 displayed satisfactory inhibition performance at 0 wt% NaCl.

It is also noticeable that Luvicap® EG performed better than Gaffix® VC-713 at lower sodium chloride concentrations. As can be seen in Figures 2.4 and 2.5, at 0.25 % of KHI, the minimum NaCl concentration required to reach more repeatable ball-stop times (>360 min) was 3 wt% for Luvicap® EG and 3.5 wt% for Gaffix® VC-713. When the KHI concentration was increased to 0.5 wt%, the minimum NaCl concentration required to reach a repeated ball-stop time of 360 min was 1.5 wt% for Luvicap® EG and 2.5 wt% for Gaffix® VC-713. Therefore, a 3.5 wt% NaCl solution was used for the rest of the study.

2.3.3 Effect of solvent concentrations on inhibition performance

The purchased Gaffix® VC-713 and Luvicap® EG contain 63% ethanol and 60% ethylene glycol, respectively. Both ethanol and ethylene glycol are effective thermodynamic inhibitors of hydrates at high concentrations. To investigate the effect of these chemicals on the ball-stop time, different amounts of ethanol and ethylene glycol were added into the THF-NaCl solutions that contained the KHIs at some concentrations equal to or below their SCCs. This was to ensure that any

synergistic effect from the added solvents would be detectable. The measured ball-stop times of these solutions are shown in Figures 2.6 and 2.7. For very low solvent concentration solutions, ethanol was first removed from Gaffix® VC-713 and then quantitatively added into the test solution in order to make the appropriate proportions of ethanol.

For 0.15 and 0.20 wt% Gaffix® VC-713 solutions (Figure 2.6), a repeatable increase in ball-stop time has been achieved by adding as little as 0.3 wt% ethanol into the system. However, at 0.075 wt%, which is much lower than the SCC (0.20 wt%), the addition of 0.3 wt% of ethanol seemed insufficient to enhance the KHI's performance.

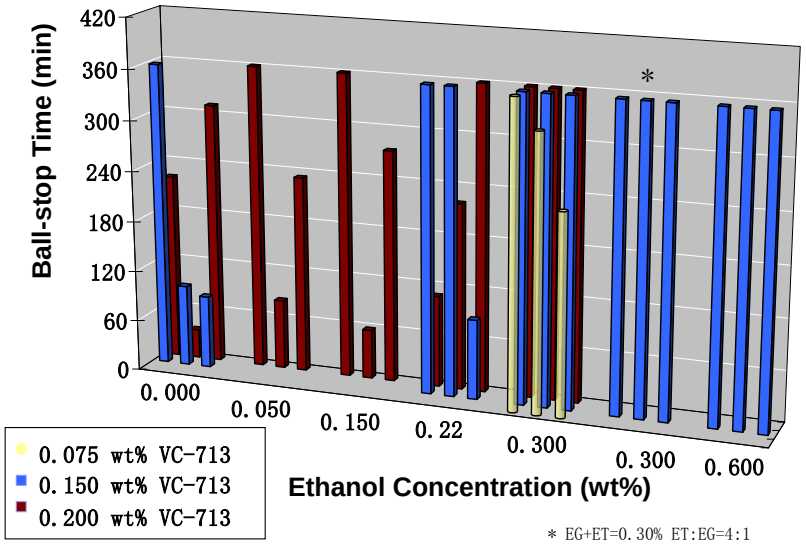

Figure 2.6 Ball-stop times for Gaffix® VC-713 (0.075 wt%, 0.15 wt%, 0.20 wt%) at different ethanol concentrations in 3.5 wt% NaCl solution

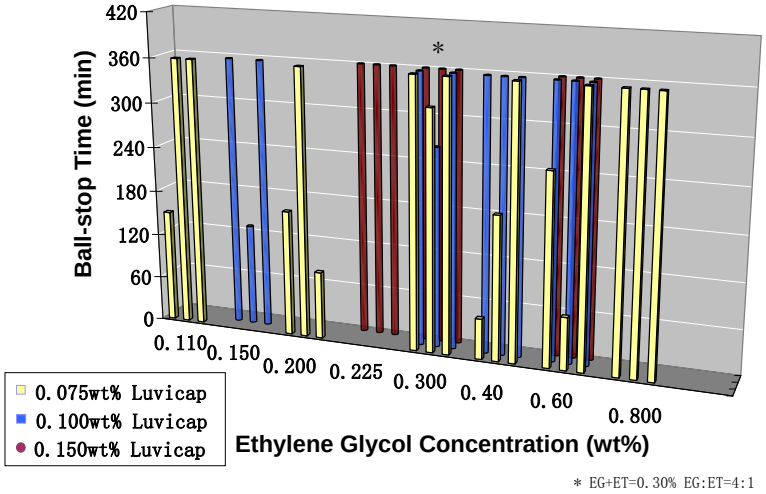

Figure 2.7 Ball-stop times for Luvicap® EG (0.075 wt%, 0.10 wt% and 0.15 wt%) at different inhibitor concentrations in 3.5 wt% NaCl solution

For 0.075 wt% Luvicap® EG, consistent ball-stop times were assured when more than 0.8 wt% ethylene glycol was added into the solution (Figure 2.7). At higher inhibitor concentrations, such as 0.1 wt%, only 0.4 wt% of ethylene glycol was needed to achieve the same result, while at 0.15 wt% of Luvicap®EG, 0.225 wt% ethylene glycol was sufficient to achieve the same result.

The above results indicate a strong synergistic effect of the solvent on the KHIs investigated. Adding a mixture of ethanol and ethylene glycol has shown similar synergistic effects as for the single solvent systems in regard to the ball-stop times (denoted by * in Figures 2.6 and 2.7). This information can be applied to current industrial operations to reduce the amount of thermodynamic inhibitors utilized.

2.4 Conclusions

The results from this chapter have demonstrated that the performance of a KHI is affected significantly by the concentration of the inhibitor, the salt strength and the presence of solvents, in particular ethanol and ethylene glycol which are utilized in the industry as thermodynamic inhibitors. A concept of specific critical concentration (SCC) has been proposed for each of the inhibitors used in this study. The SCC value is dependent not only on the type of KHI, but also on the additives in the test solutions, such as salts and solvents. Evaluation and comparison of the inhibition performance of different KHIs should consider only the measured results at equal to or above their SCCs. Salt and solvent concentrations and other additives present in the operating systems must be considered when a suitable concentration is determined for the field application of a particular KHI. Studies on interfacial activities of these polymers have shown similar critical concentrations that affect the surface tension of a system.

Many problems were encountered in this work. The most significant problem is that the ball-stop times observed from the rig test experiments were not always consistent or reproducible. Through the study carried out in this chapter, we found that the rig testing provided reliable information only if the concentration of the inhibitor was above its SCC, below which the test results scattered drastically and were inconsistent.

CHAPTER 3 Investigation of Luvicap® EG and Gaffix® VC-713 using rheological method

3.1 Introduction

In the previous chapter, the effects of various concentrations and the synergistic effect of salt and organic solvents on the inhibition performance of selected inhibitors were studied, using a ball-stop rig at a constant temperature of 0 ℃, which is below the THF hydrate-forming temperature of 4.4 ℃. The parameter used for the evaluation was ball-stop time, which indicates the time taken for hydrates to fully plug the system in a test tube. The concept of specific critical concentration (SCC) has been proposed for a KHI performance study. Below SCC, the inhibition performance of an inhibitor is generally poor and the testing results are not reproducible. Above this critical concentration, inhibitors show good and reproducible performance.

In this chapter, the same THF hydrate-forming process is investigated under dynamic conditions, with changing temperature, by the use of a rheometer. This investigation was carried out in order to understand the hydrate-forming process in the presence of selected inhibitors, with changes in inhibitor concentrations and temperatures. The induction time and temperature at which THF hydrates start to form are explored.

3.1.1 General principle of rheology

Rheology is the discipline which was formally proposed to describe “the study of the flow and deformation of all forms of matter” by E.C Bingham and M. Reiner in 1929. The word rheology was created by E.C Bingham using the Greek roots of "rheo", meaning "everything flows", and "-ology", meaning "the study of" (Morrison, 2001). Thus, rheology is the science of the deformation and flow of materials. In principle, rheology includes everything dealing with flow behaviour: aeronautics, hydraulics, fluid dynamics and, even, solid mechanics. The principal theoretical concepts are: kinematics, dealing with geometrical aspects of deformation and flow; conservation laws, dealing with forces, stresses and energy interchanges; and constitutive relations, special to classes of bodies (Morrison, 2001). However, in practice, rheology has usually been restricted to the study of the fundamental relations, called constitutive relations, between force and deformation in materials, primarily liquids(Macosko, 1994).

Generally, measurements of rheology have been conducted by imposing a specific stress field or deformation to the sample fluid, and monitoring the resultant deformation or stress. There are three configurations commonly used for rheological measurements. A brief description of each of these configurations is given below.

(1) Pipe or Capillary: The test liquid is forced through a tube of constant cross-section and precisely known dimensions under conditions of laminar flow. Either the flow rate or the pressure drop is fixed and the other is measured. Knowing the dimensions, the flow rate can be converted into a value for the shear rate, and the pressure drop into a value for the shear stress. This method is widely used for measuring viscous fluids, such as asphalt cements, polymer melts and stable concentrated suspensions. This method has the advantage of high precision and simple design, and is less subject to temperature effects that can occur during shearing of highly viscous fluids in rotational devices. Figure 3.1 is a schematic diagram of a capillary rheometer. By measuring the pressure drop across the capillary as a function of flow rate for multiple capillaries of the same diameter, d, but differing length, L, it is possible to determine the viscosity as a function of shear rate. (Sherman, 2004, Malkin and Isayev, 2006, Clegg and Collyer, 1998)

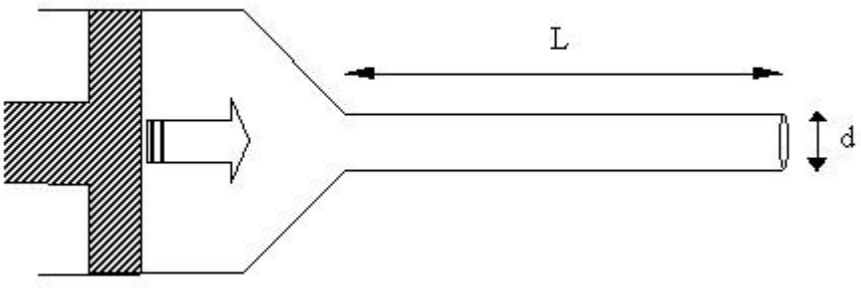

Figure 3.1 Schematic diagram of a capillary rheometer

2) Rotational cylinder: The test liquid is deposited within the space between one cylinder placed inside another. One of the cylinders is rotated at a set speed. This determines the shear rate inside the annulus. The liquid tends to drag the other cylinder round. The force it exerts on that cylinder (torque) is measured and, later, converted to a shear stress value. In a rotational cylinder rheometer, either the inner, outer or both cylinders may rotate, depending on instrument design. The test fluid is maintained in the annulus between the cylinder surfaces. A rotational cylinder rheometer is useful for low viscosity fluids, as it has a large total surface area, creating viscous drag on the rotating inner cylinder, which generally increases the accuracy of measurements. Figure 3.2 is a schematic diagram of the rotational cylinder rheometer. (Sherman, 2004, Malkin and Isayev, 2006, Clegg and Collyer, 1998)

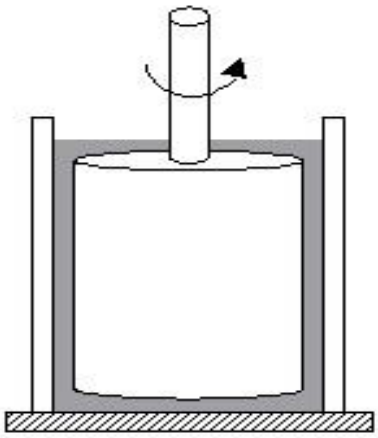

Figure 3.2 Schematic diagram of rotational cylinder rheometer

(3) Cone and plate: The cone and plate rheometer consists of an inverted cone in near contact with a lower plate. The cone is usually designed with an angle of less than 4 º. Either the upper or lower surface may rotate, depending on instrument design. Another form with parallel plate geometry can be considered as a simplified version of the cone and plate, but having an angle of 0 º. The test liquid is deposited on a horizontal plate and a shallow cone is placed into it. The test fluid is constrained in the narrow gap between the two surfaces. Typically, the plate is rotated and the force on the cone is measured. The movement of the cone is resisted by a thin piece of metal which twists - known as a torsion bar. The known response of the torsion bar and the degree of twist give the shear stress, while the rotational speed and cone dimensions give the shear rate. Both the cone and plate and the parallel plate measurement tools are most often used for highly viscous pastes, gels and concentrated suspensions. Figure 3.3 is a schematic diagram of the cone and plate rheometer.

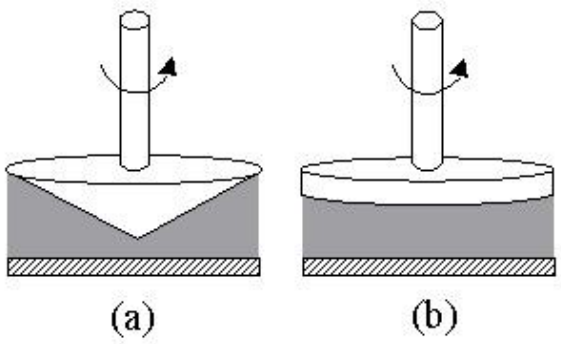

Figure 3.3 Schematic diagram of cone and plate rheometers:

(a) cone and plate, (b) parallel plate

3.1.2 Application of rheology in gas hydrates

Rheology is of high value in the study of material properties and process analysis, therefore it has wide applications in materials science and engineering, geophysics, physiology, human biology and pharmaceutics. In flow assurance of oil transportation lines, rheology analysis of hydrate slurry has been used for prediction of the hydrate transportation capabilities of oils under realistic production conditions (Hald and Nuland, 2007). Rheological methods also have been used for hydrate detection and characterization (Schuller et al., 2005). In addition, rheology has been used as an effective method to study hydrate formation, dissociation and aggregation (Rensing et al., 2008). As a typical material deformation measurement, the rheological method also has been used for analysis of the hydrate inhibition process, by monitoring the flow behaviours of clathrate hydrate slurries or hydrate-forming fluids (Rensing et al., 2008, Delahaye et al., 2011, Peixinho et al., 2010, Fidel-Dufour et al., 2006). Rheological properties, such as viscosity and yield stress, and the temperature effect on these parameters, can be measured to study the phase change processes of hydrate slurries and hydrate-forming fluids (Delahaye et al., 2011, Peixinho et al., 2010, Fidel-Dufour et al., 2006).

Rheology also has been shown to be an effective and informational tool for analysing clathrate hydrate formation and aggregation. For example, the nucleation and aggregation of methane hydrate was clearly observed in both shear

and oscillatory time sweep experiments under the condition of being cooled from 20 °to 0 ℃ (at a rate of 0.5 ℃/minute) and a pressure of approximately 9.5 MPa (Rensing et al., 2008). Rheological methods also have provided a novel way to detect clathrate hydrate dissociation (Rensing et al., 2008). Besides being effective and informational, there are some other advangates of rheological measurements, such as easy aquisition and low up-front investment, which have attacted researchers' interests to develep a good rheological methold for the investigation of hydrates.

3.1.3 The method for this study

In this research, a rotational cylinder rheometer was used to study the inhibition behaviour of Gaffix® VC-713 and Luvicap® EG of varying concentrations when the test solutions were cooled from room temperature to -5 ℃ at an approximate cooling rate of 2 ℃/min. The changes in shear stress and temperature of the sample during the entire hydrate forming process were monitored. Based on the shear stress history and temperature history, it was possible to determine the induction time and temperature at the formation of THF hydrates.

3.2 Experimental

3.2.1 Chemicals and materials

Details of chemicals are supplied in section 2.2 of Chapter 2.

3.2.2 Rheometer setup

The equipment system used for this study was a Haake Modular Automate Rheometer MARS II (Figure 3.4), with a PZ 38 pressure cell (Rotor PZ 38, D = 38 mm, L = 93mm, made of stainless steel) (Figure 3.5) and a temperature controller. A thermal sensor was connected to the pressure cell to record the temperature history of the test sample. The testing temperature was controlled by a cooling system. The shear stress and temperature history were automatically acquired using the operating software of the rheometer.

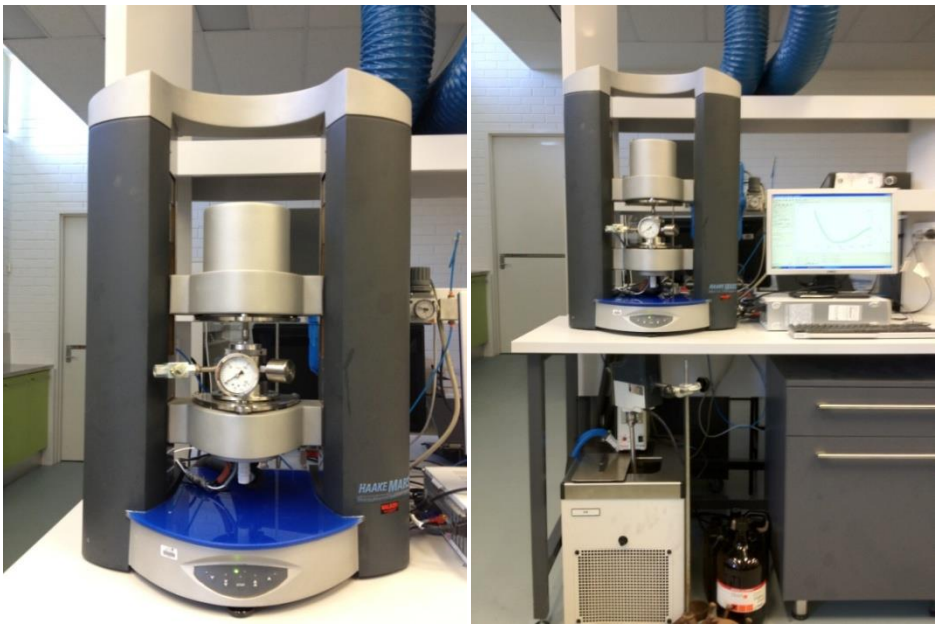

Figure 3.4 Haake Modular Automate Rheometer II

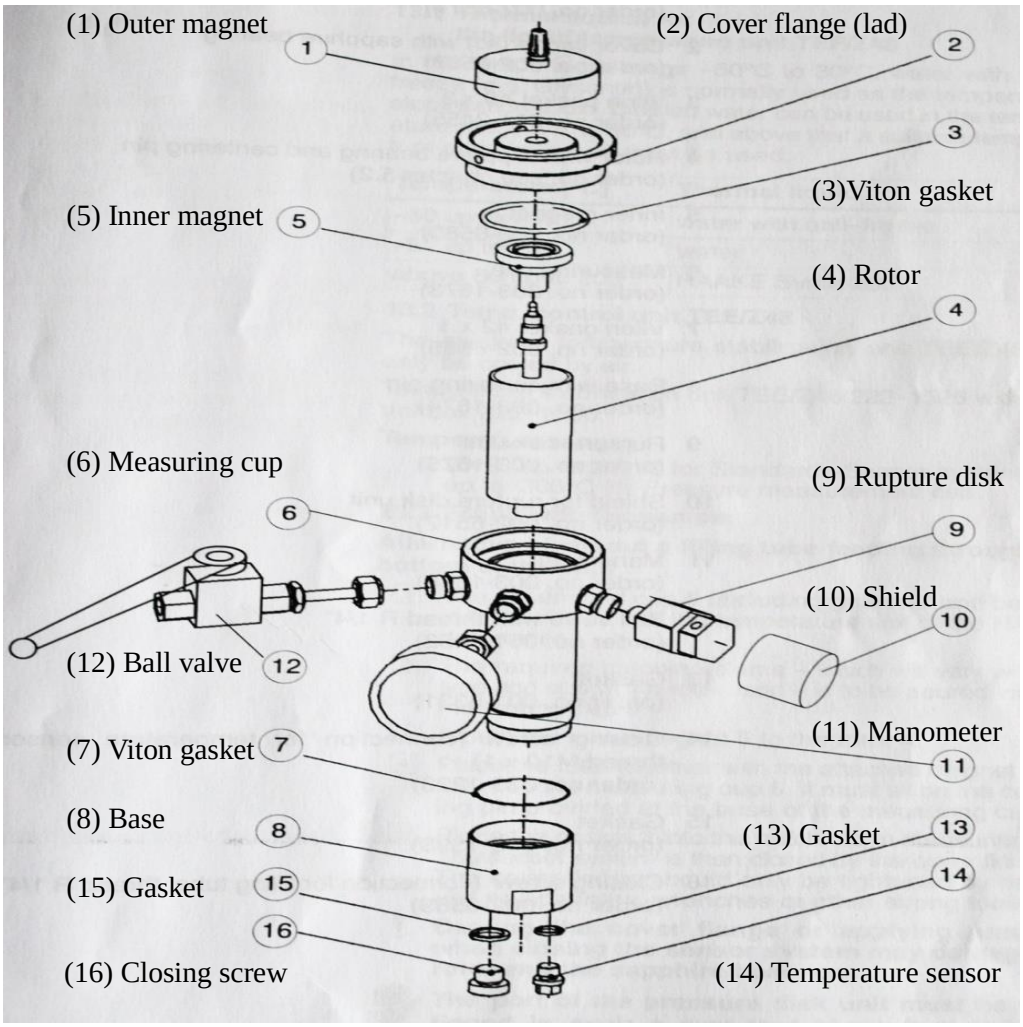

Figure 3.5 Schematic diagram of PZ38 pressure cell (top) and a photo of the assembled cell (bottom)

In this set up, the pressure cell provides a sealed space for rheological measurement. Referring to the schematic of Figure 3.5, the assembled measuring cup **6** (including gasket **7** and base **8**) is to be placed into the temperature unit of the Haake rheometer. The required sample volume is to be poured into the measuring cup **6**. The inner magnet **5** is attached to the rotor **4** and the rotor, together with the attached magnet, is placed carefully into the measuring cup. It must sit on the centring pin provided at the base **8** of the measuring cup. The gasket **3** is placed into the notch of the measuring cup. The sensor system is then sealed by the cover flange **2**. The cover flange should only be tightened by hand (no use of spanners, wrenches or other strong tools). Finally the outer magnet **1** of the pressure cell is attached. During the testing, the outer magnet drives the inner magnet's movement by magnetic force, and shear stress is detected by the Haake rheometer motor that is attached to the outer magnet.

The schematic of the rheology system is shown in Figure 3.6. A cylinder/rotor rheometer with temperature controller was used to create a hydrate-forming environment in which to monitor the hydrate-forming process of the sample solution. Experimental data were collected by a computer equipped with the control software (HAAKE RheoWin version 3.61.0000) of the rheometer. A small piece of elastic stainless steel wire (shown in Figure 3.7) was fixed onto the base of the measuring cup of the pressure cell. The gentle scratching of the surface of the rotor by the wire created a constant crystallization-initiating force in the

hydrate-forming liquid.

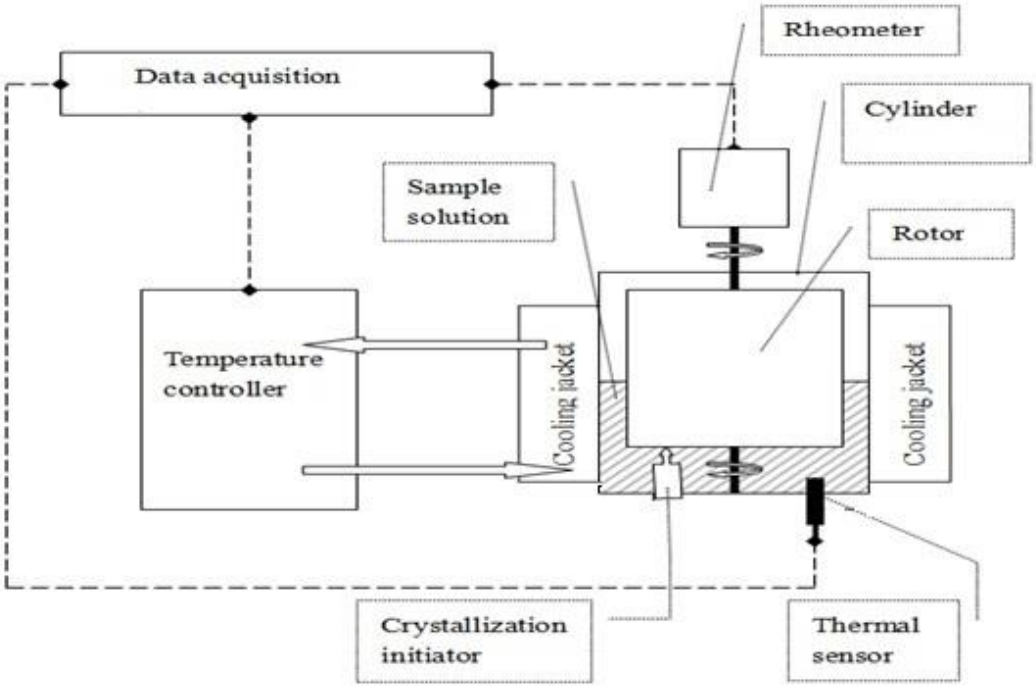

Figure 3.6 Schematic diagram of Rheological hydrate-inhibitor evaluation system

Figure 3.7 Elastic stainless steel wire fixed onto the bottom of the cylinder as a crystallization initiator

3.2.3 Sample preparation

Sodium chloride stock solutions and test solutions were prepared using the same procedure described in section 2.2 of Chapter 2. The investigated concentrations of Luvicap® EG and Gaffix® VC-713 and the test conditions are summarized in Table 3.1. Environmental temperature, $T_{e,}$, denotes the set temperature to which a testing solution was cooled during the measurement.

Table 3.1 THF hydrate-forming solution for rheological investigation

NaCl (wt%)	KHIs (wt%)		Environmental Temperature (℃)
	Gaffix®VC-713	Luvicap® EG	
3.5	0	0	0, -5
	0.1	0	-5
	0.3	0	-5
	0.5	0	-5
	0.7	0	-5
	1.0	0	-5
	1.5	0	-5
	0	0.1	-5
	0	0.2	-5
	0	0.3	-5
	0	0.5	-5
	0	0.7	-5

3.2.4 Rheological testing

The rheometer was set up in the controlled rate (**CR**) mode for the test. All rheological testing works were conducted with a constant shear rate of 200/sec. The cooling system was set up at -5 °C, unless otherwise specified. Prior to the testing, the temperature of the pressure cell was brought to T_e and equilibrated for 1.5 hours at T_e. When the setup was ready, 20 ml of test solution was transferred into the measuring cylinder of the pressure cell. Rotation started immediately, however, data collection started only after the sample temperature had reached 8 ℃. The time at which data collection started was set as **Time Zero**, $t_0 = 0$ sec. The testing was stopped when the cylinder was totally plugged with hydrates, which could be observed from the shear stress curve (for details, see the following section) or at t = 4 hours if no full blockage was observed before that. Between each individual test, the sample cell and rotor were washed with deionised water and dried in air.

3.3 Results and discussion

3.3.1 Observation of the THF hydrate-forming process

Shown in Figure 3.8 is the shear stress history and temperature history of a THF-Water solution (1:3v/v) when T_e was set at 0.0 ℃. There is no inhibitor in this hydrate-forming system.

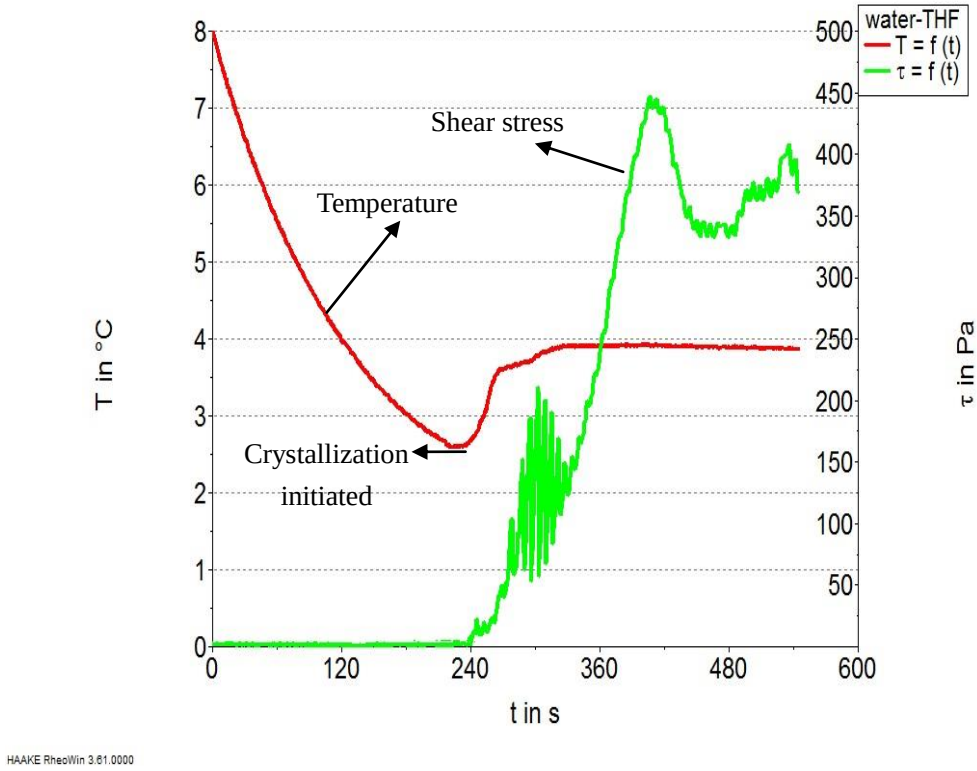

Figure 3.8 Rheological observation of THF-Water

Figure 3.8 shows that the sample temperature decreased monotonically at the beginning. A sudden rise in temperature from 2.6 ℃ to 3.8 ℃ was recorded at 230 sec, indicating the start of hydrate formation. Therefore, the **induction time** of this hydrate-forming solution is considered to be $t_i = 230$ sec, and the **onset temperature** $T_{onset} = 2.6$ ℃, which is 1.8 ℃ below the equilibrium temperature of

the THF hydrate in THF: Water (1:3 v/v) environment (4.4 ℃ at atmospheric pressure). As crystallization starts, heat is released, which results in the temperature rise. The increase in temperature became much slower after it had reached 3.8 ℃. The temperature reached a plateau at about 4.0 ℃, at 330 sec, which is quite close to the equilibrium temperature of the THF hydrate. Shear stress also increased dramatically during this period, due to rapid hydrate formation. It reached the maximum value of 445 Pa at 420 sec, indicating a total plugging by THF hydrates in the sample cell. The time at which the maximum shear stress was reached is defined as **time of total plugging** (t_{tp}) and **maximum shear stress** as $\tau_{max.}$ For the THF hydrate-forming solution containing no KHIs, t_{tp} = 420 sec and τ_{max} = 445Pa. The observed time taken for the rapid shear stress increase was longer than that for the temperature increase (from 230 sec to 290 sec). This indicates that hydrate crystals continued their growth until 420 sec, however the released heat had been compensated by the forced cooling of the system. It is also possible that most THF had been consumed and converted into hydrates before 290 sec, followed by aggregation of the formed THF hydrates. There was a drop of shear stress after the shear stress reached τ_{max}, which was due to the detachment of the hydrates blockage from the surface of the rotor. It also indicated that the test sample had formed a big blockage of hydrates. Photographs of the formed THF hydrates in the test cell are displayed in Figure 3.9

Figure 3.9 THF hydrates, formed in the pressure cell

Table 3.2 summarizes the parameters that were used to interpret the rheological testing results. These parameters for all test samples were collected and the results were compared.

Table 3.2 Parameters used for interpretation of rheological observations

Parameter	Definition	Physical meaning
T_e (℃)	Environmental temperature	The desired end temperature chosen for the measurement
t_i (sec)	Induction time	The time at which hydrates start to form
T_{onset} (℃)	Onset temperature	The temperature of the sample at which hydrates start to form
τ_{max} (Pa)	Maximum shear stress	The shear stress at which the maximum value and full blockage were observed
T_{tp} (sec)	Time of total plugging	The time at which total plugging was observed

A test of another blank solution was conducted. Figure 3.10 shows the temperature and shear stress curves against time. It can be seen that the curves obtained from these two experiments are generally close to each other without many differences. A summary of the observed data is given in Table 3.3. It further demonstrates that the testing is reproducible for the testing of other hydrate-forming solutions. Only one set of experiments was conducted.

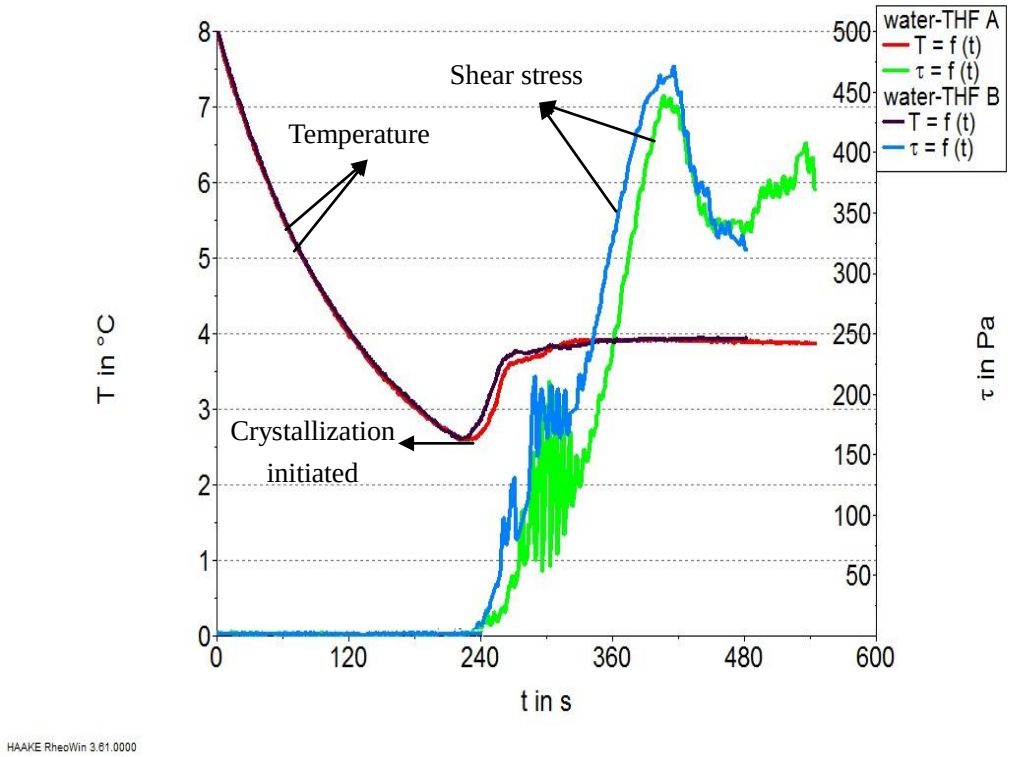

Figure 3.10 Validation of rheological setup

Table 3.3 Rheological observation of two replicates of the same hydrate-forming solution

Sample	**t_i (sec)**	**T_{onset} (℃)**	**τ_{max} (Pa)**	**t_{end} (sec)**
Water-THF A	230	2.6	450	420
Water-THF B	225	2.6	475	420

3.3.2 Investigation of Gaffix® VC-713

The hydrate-forming solutions containing Gaffix® VC-713 in concentrations of 0.1 %, 0.3 %, 0.5 %, 0.7 %, 1.0 % and 1.5 % were tested. The T_e was set at -5 ℃ for the THF hydrate-forming solution in the presence of KHIs during the testing. This temperature was selected after a few trials to ensure that THF hydrates formed within the parameters for all selected KHI concentrations. Figure 3.11 shows the temperature history and shear stress history of the THF hydrate-forming solution in the presence of 0.5 % Gaffix® VC-713. The curves show a similar pattern to the THF hydrate-forming solution containing no inhibitors (Figure 3.10).

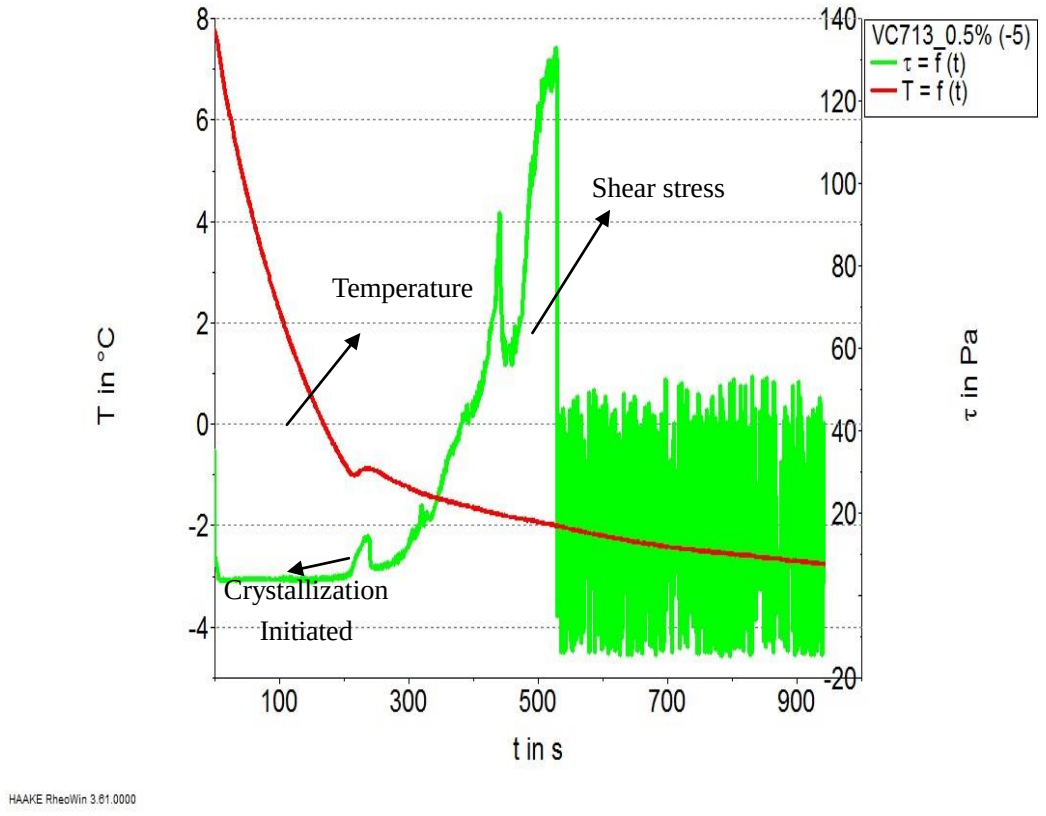

Figure 3.11 Rheological observation of the performance of Gaffix® VC-713

In general, the temperature of the hydrate-forming solution decreased smoothly from 8 ℃ to -1.1 ℃ whilst shear stress stayed constantly at 5 Pa until $t_i = 205$, when a turning point was observed, due to the formation of THF hydrates. The onset temperature was $T_{onset} = -1.1$ °C. Correspondingly, the shear stress started to increase, reflecting the flow behaviour change of the samples due to the formation of THF hydrates. It can be seen that, between 205 and 565 sec, the shear stress of the sample increased dramatically from 5 Pa to 200 Pa, indicating the formation of hydrate blockages. There was a fluctuant pattern of shear stress after 565 sec, which was due to the detachment of the hydrates blockage, with the surface of the rotor deconstructed by high shear stress.

Temperature histories and the shear stress history of all tested solutions are displayed in Figures 3.12 and 3.13. The measured parameters are summarized in Table 3.4. It can be seen that a higher concentration of the inhibitor results in lower T_{onset} and longer t_i. For example, when there was no Gaffix® VC-713 present in the THF hydrate-forming solution, hydrates started forming as soon as the temperature reached 1.1 ℃. However, when Gaffix® VC-713 was present in the solution, T_{onset} was reduced to 0.0 ℃, -0.4 ℃, -1.1 ℃, -1.5 ℃, -3.3 ℃ and -4.1 ℃, respectively, as increasing concentrations of the inhibitor were added to the solution. The induction times of these solutions were 130 sec, 180 sec, 202 sec, 215 sec, 280 sec, 290 sec and 600 sec, respectively, with 0.1 %, 0.3 %, 0.5 %, 0.7 %, 1.0 % and 1.5 % Gaffix® VC-713. There was a significant time increase

for t_i between the 1.0 % and 1.5 % Gaffix® VC-713 hydrate-forming solutions. This is probably due to the synergistic effect of ethanol. The Gaffix® VC-713 used during the test was 37 % solution (in ethanol), so the 1.0 % and 1.5 % Gaffix® VC-713 hydrate-forming solutions contained 1.7 % and 2.6 % ethanol, respectively. Results of the synergistic effect of KHIs studied by other team members in our group have shown that ethanol significantly improves the inhibition performance of Gaffix® VC-713 only when its concentration is over 2 %. This additional information explains the above phenomenon.

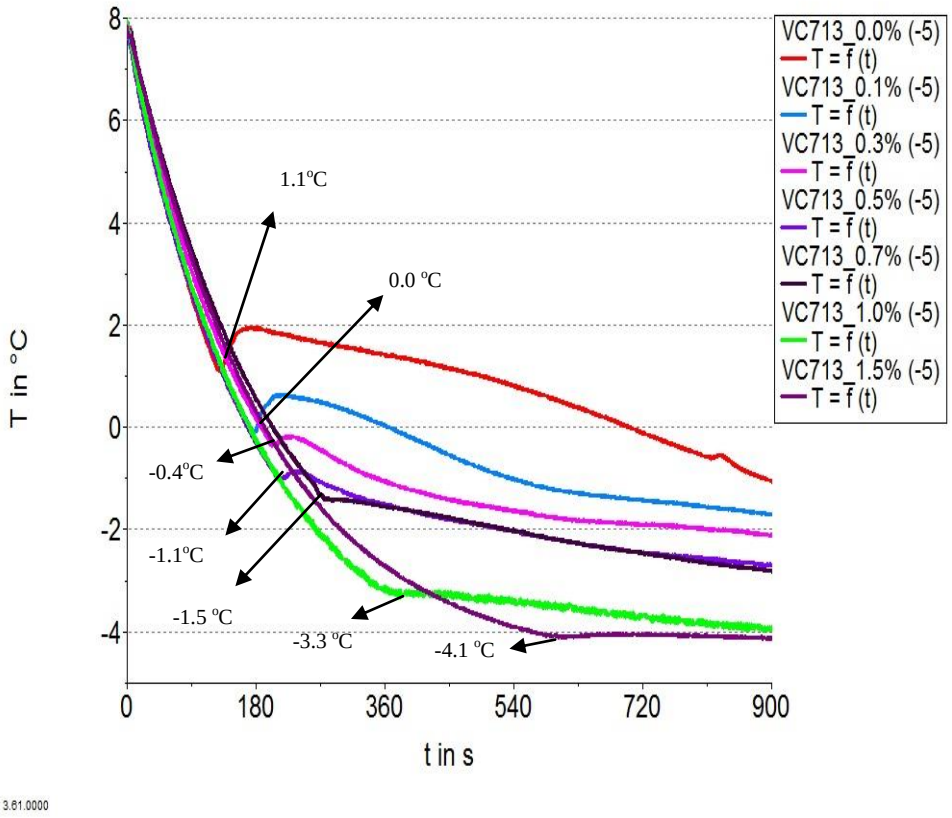

Figure 3.12 Temperature histories of Gaffix® VC-713in various concentrations

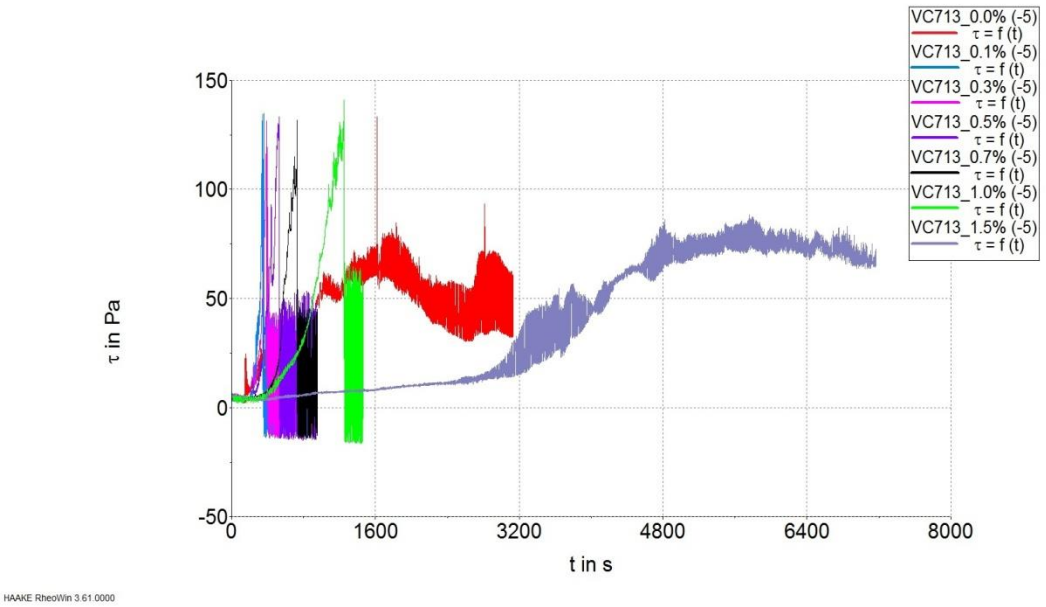

Figure 3.13 Shear stress histories of Gaffix® VC-713in various concentrations

Table 3.4 Parameters of hydrate-forming solutions with various Gaffix® VC-713 concentrations

Gaffix®VC-713 (wt%)	t_i (sec)	T_{onset} (℃)	τ_{max} (Pa)	t_{tp} (sec)
0.0	130	1.1	133	1,650
0.1	180	0.0	134	345
0.3	202	-0.4	132	390
0.5	215	-1.1	133	527
0.7	280	-1.5	132	728
1.0	290	-3.3	141	1,253
1.5	600	-4.1	87	4,800

The total plugging time (t_{end}) increased from 345 sec to 4,800 sec with increase of Gaffix® VC-713 concentration from 0.1 % to 1.5 %. It is interesting to note that the 0.0 % Gaffix® VC-713 solution produced t_{end} = 1,650 sec, which is greater in

value than almost all tested solutions apart from that containing 1.5 % Gaffix® VC-713. It is believed that this phenomenon was due to the T_{onset} of 0.0 % Gaffix® VC-713 hydrate-forming solution being as high as 1.1 ℃, which was close to the equilibrium temperature of hydrate formation in THF : 3.5 % NaCl (1:3 v/v) environment (~2 ℃). Therefore, the hydrate crystals appeared to have a low growth rate.

3.3.3 Investigation of T_{onset} on Gaffix® VC-713

Onset temperature has been used frequently to describe the hydrate forming process, by many researchers (Zhang et al., 2004, Rensing et al., 2008). It reflects the minimum temperature at which a hydrate-forming solution remains in pure liquid phase. When the temperature is below its T_{onset}, the hydrates form rapidly regardless of the presence of inhibitors. Significant kinetic behaviour of an inhibitor is observable when the sample temperature is above its T_{onset}. Therefore, the onset temperature is dependent not only on the type of inhibitor but also on the inhibitor concentration. In order to prove this hypothesis, a further test was conducted on a THF hydrate-forming solution containing either 0.1 % or 0.5 % of Gaffix®VC-713. The tests were carried out at $T_e = T_{onset}$ +/- 1.0 ℃ respectively. The results are shown in Figures 3.14 and 3.15.

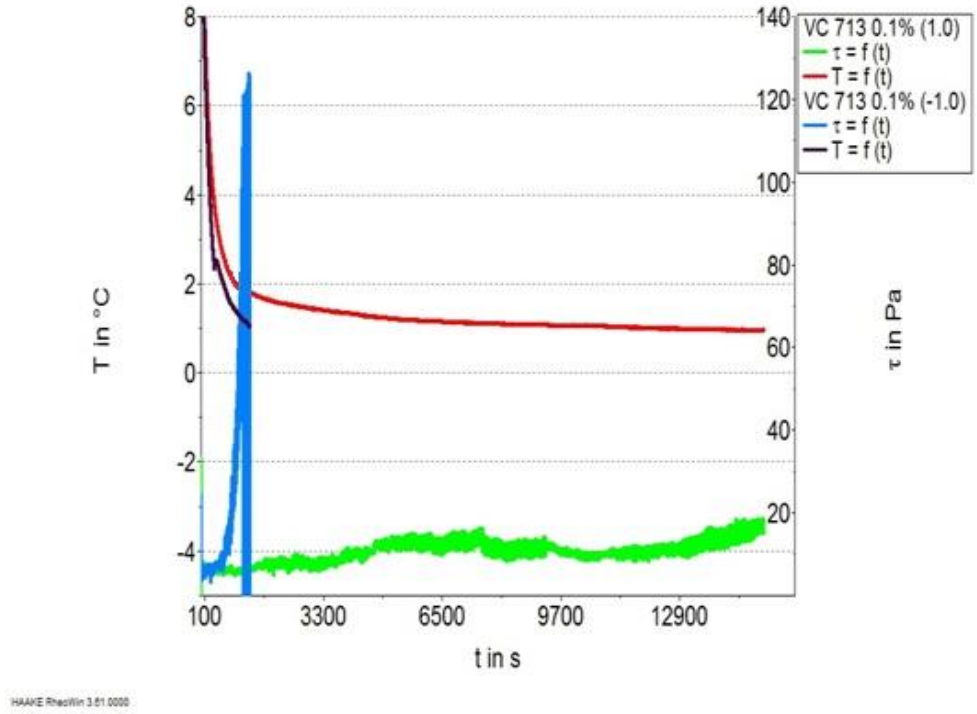

Figure 3.14 0.1 % Gaffix® VC-713 hydrate-forming solution at T_e = -1.0 ℃ and T_e = 1.0 ℃

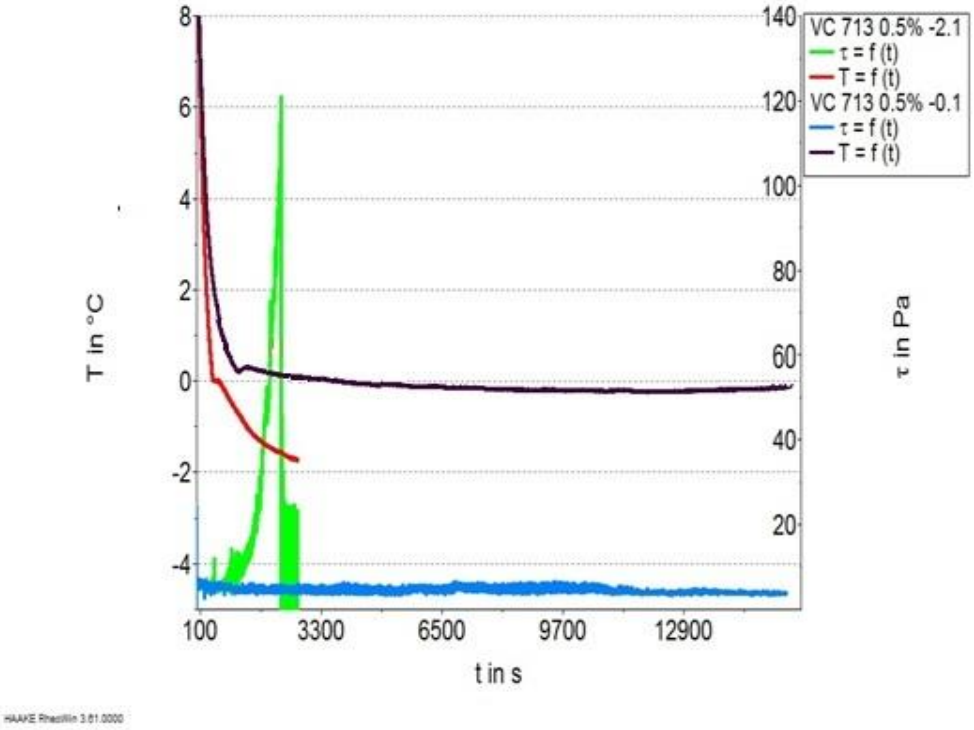

Figure 3.15 0.5 % Gaffix® VC-713 hydrate-forming solution at T_e = -2.1 ℃ and T_e = -0.1 ℃

For the THF hydrate-forming solution containing 0.1 % Gaffix® VC-713, when T_e = -1.0 ℃, which is 1.0 ℃ lower than T_{onset} (0.0 ℃), a full hydrates blockage was seen at t_{tp} = 1,080 sec and τ_{max} = 128 Pa (Figure 3.14). The de-assembled measuring cylinder, with formed hydrates, was photographed and is shown in Figure 3.16. At T_e = 1.0 ℃, which is 1.0 ℃ higher than T_{onset}, no significant increase in shear stress was observed, i.e. there was no plugging observed over 4 hours (Figure 3.14). However, a small amount of hydrate crystal formation was found in the testing cylinder (Figure 3.17), indicating that the formation of hydrates occurred, but the presence of inhibitors had delayed the total plugging of the test cell. This is how a KHI works: it can delay and slow, but not stop, the formation of hydrate.

Figure 3.16 Hydrates block formed in a Gaffix® VC-713 sample at T_e = -1.0 ℃

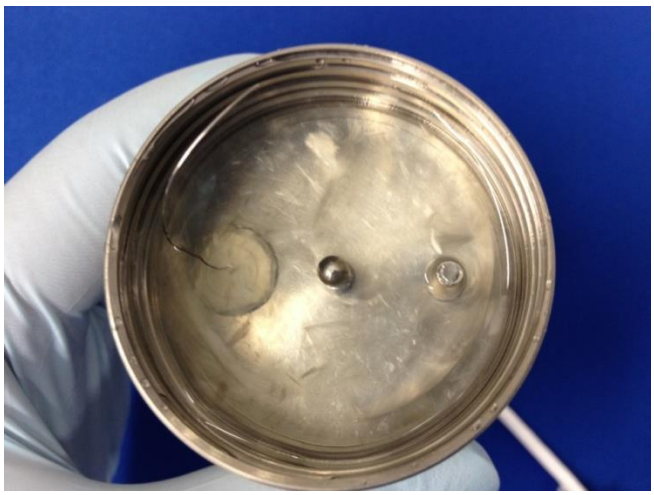

Figure 3.17 Post-testing sample of 0.1 % Gaffix® VC-713 solution at T_e = 1.0 ℃

In Figure 3.14, spikes can be observed in the temperature curve of T_e = -1.0 ℃ (0.1 % Gaffix® VC-713). It is believed that those spikes were the result of homogeneous nucleation of THF hydrates. Similar observations have been reported by Zhang et al (2004) in their studies of hydrates using differential scanning calorimetry. The authors claimed that the spikes occur at different temperatures, indicating they are random in nature. There were no observations of spikes for homogeneous nucleation in the temperature curve of T_e = -5.0 ℃ (Figure 3.12). This is because the high cooling rate resulted in the spike of the nucleation overlapping the peak of T_{onset}. Figure 3.18 represents the relationship between cooling rate and resolution of temperature curves, which was obtained by other researchers.

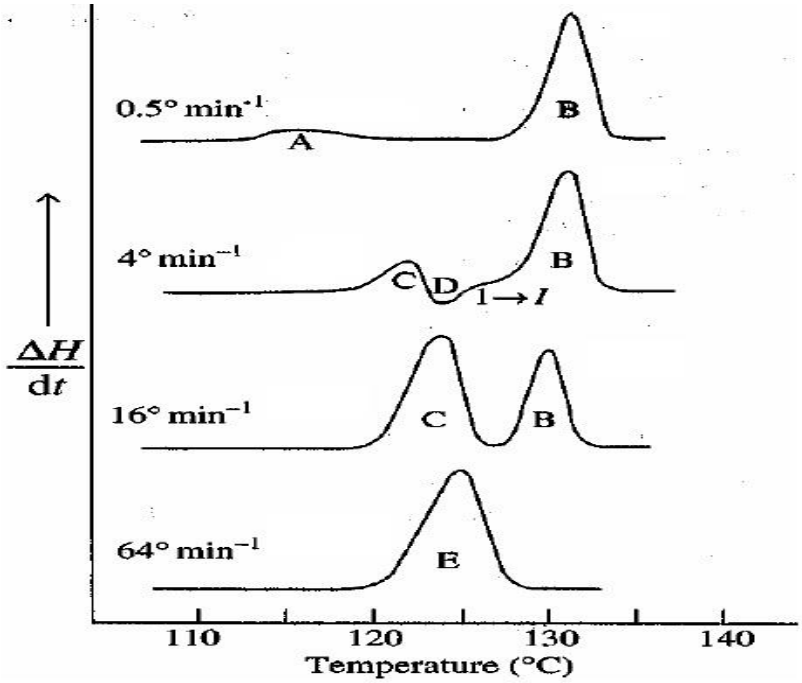

Figure 3.18 Relationship between cooling rate and resolution of temperature curves (Claire, 2006)

Similar results were obtained for the hydrate-forming solution containing 0.5 % Gaffix® VC-713 (Figure 3.15). At T_e = -2.1 ℃, which is 1.0 ℃ lower than T_{onset} (-1.1 ℃), blockage and rapid formation of hydrates were observed at t_i = 270 sec and total plugging at t_{tp} = 2,250 sec. When T_e = -0.1 ℃, which is 1.0 ℃ higher than T_{onset}, no blockage was observed over 4 hours. Spikes in homogeneous nucleation also have been observed. Photographs were taken of the samples after testing. The photograph shown in Figure 3.19 is of the hydrates blockage removed from the measuring cylinder of the 0.5 % Gaffix® VC-713 at T_e = -2.1 ℃ test. The photograph shown in Figure 3.20 illustrates the post-testing sample of 0.5 % Gaffix® VC-713 at T_e = -0.1 ℃ in the measuring cell. No hydrates were seen on the testing cylinder.

Figure 3.19 Hydrate blockage formed in 0.5 % Gaffix®VC-713 test at T_e = -2.1 ℃

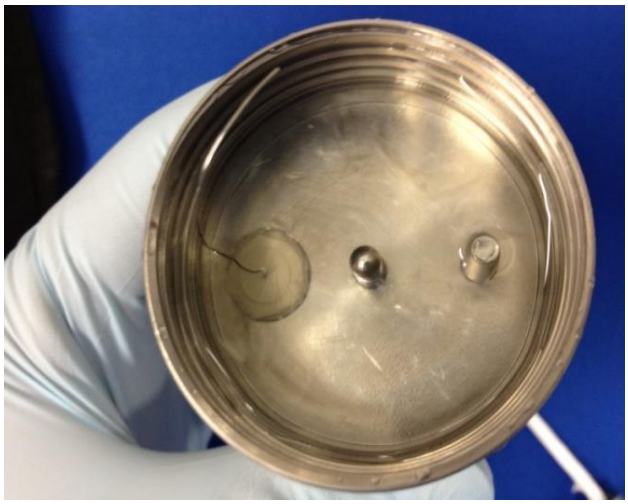

Figure 3.20 Post-testing sample of 0.5 % Gaffix® VC-713 solution at T_e = -0.1 ℃

3.3.4 Investigation on Luvicap® EG

A series of hydrate-forming solutions containing varying concentrations of Luvicap®EG also were tested at T_e = -5.0 ℃. The inhibitor concentrations were reported previously in Table 3.1. Figure 3.21 shows the temperature history and shear stress history of the THF hydrate-forming solutions in the presence of 0.5 % Luvicap® EG. The hydrate-forming process is similar to that of 0.5 % Gaffix® VC-713.

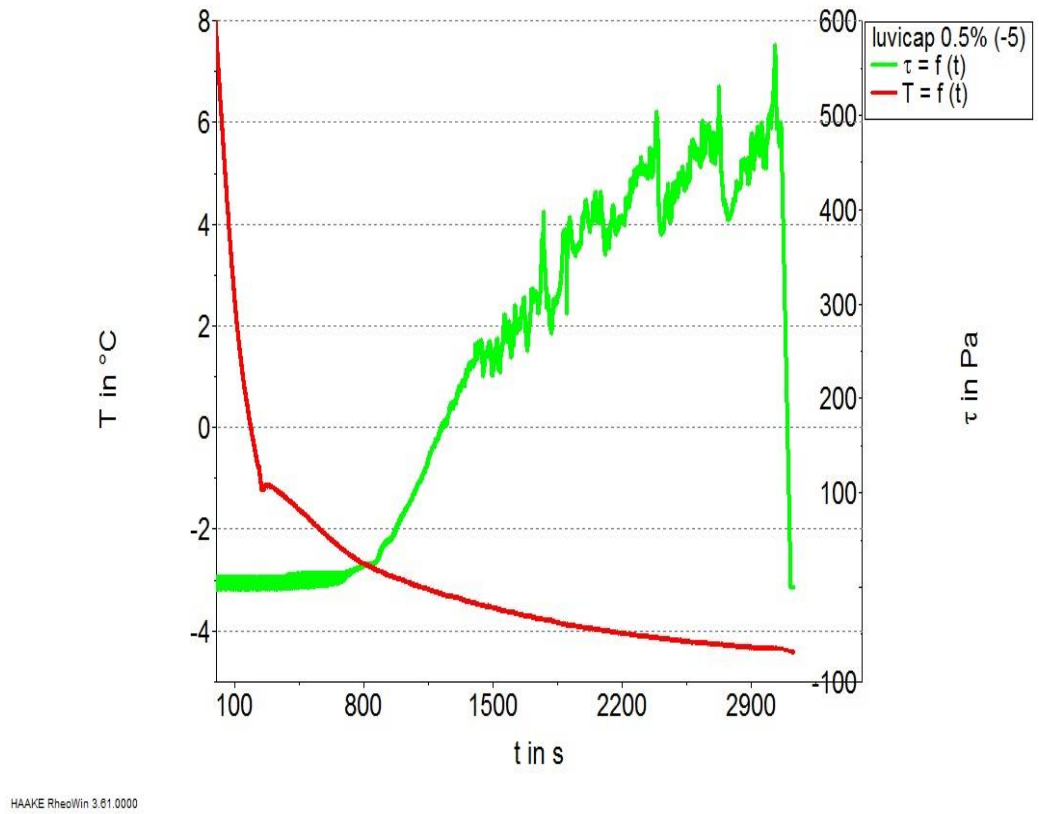

Figure 3.21 Rheological observation of Luvicap® EG performance at T_e = -5 ℃

However the key parameters vary depending on KHIs and their concentrations. The temperature histories and shear stress histories of all measured samples are

displayed in Figures 3.22 and 3.23, for comparison. The key parameters of the hydrate formation process are tabulated in Table 3.5.

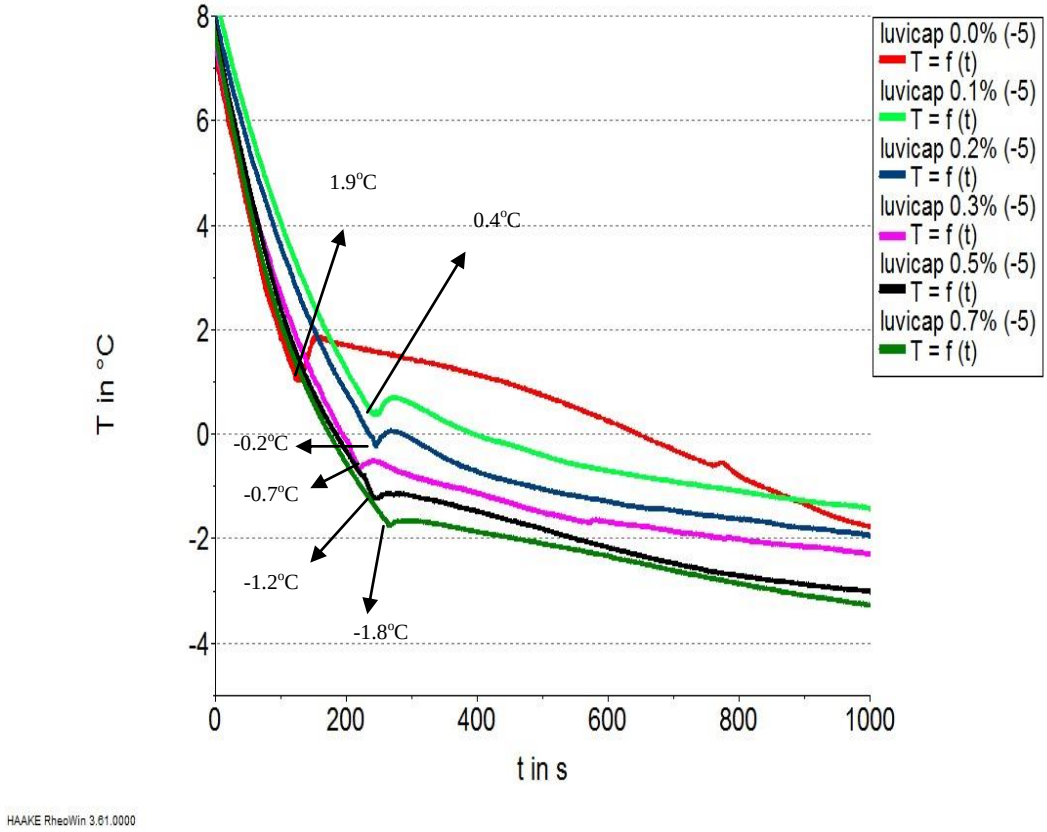

Figure 3.22 Temperature histories of Luvicap® EG in various concentrations

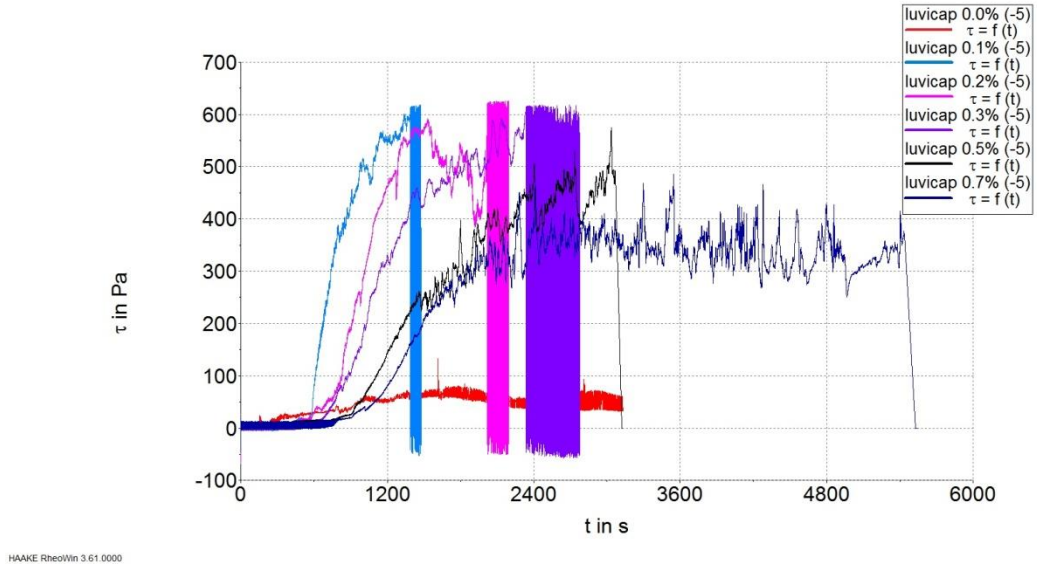

Figure 3.23 Shear stress histories of Gaffix® VC-713in various concentrations

Table 3.5 Parameters of THF hydrate-forming solutions with various Luvicap®EG concentrations

Luvicap® EG	**t_i (S)**	**T_{onset} (℃)**	**τ_{max} (Pa)**	**t_{tp} (S)**
0.0	130	1.1	133	1,650
0.1	230	0.4	610	1,330
0.2	237	-0.2	620	2,020
0.3	210	-0.7	615	2,270
0.5	240	-1.2	575	3,000
0.7	257	-1.8	470	2,350

These results demonstrate that the higher is the Luvicap® EG concentration, the lower is the T_{onset} value obtained, which is the same result as that observed in Gaffix®VC-713. However, the hydrates' induction time (t_i) was almost the same for all tested samples, as was the total plugging time (t_{tp}). The Luvicap® EG used was a 40 % solution in ethylene glycol. According to results of the synergistic effect of KHIs studied by the other team members in our group, ethylene glycol significantly improves the inhibition performance of Luvicap® EG when its concentration is over 0.3 %. The 0.2 % Luvicap® EG hydrate-forming solution contains 0.3 % ethylene glycol. That is why there was no considerable increase in $t_{i,}$ when the Luvicap® EG concentration was increased from 0.2 % to 0.7 %. It also was found that the τ_{max} values of Luvicap® EG samples (approximately 600 Pa) were much higher than the τ_{max} values of Gaffix® VC-713 samples (approximately 130 Pa). It is believed that this phenomenon indicates that

Luvicap® EG samples form more solid hydrate blockages than Gaffix® VC-713 samples. This needs more future work to investigate this assumption.

Results also show that Luvicap® EG produced a better inhibition performance than Gaffix® VC-713. The t_i of Luvicap® EG was generally longer than the t_i of Gaffix® VC-713, and T_{onset} (Luvicap® EG) was lower than T_{onset} (Gaffix® VC-713). This means that Luvicap® EG has better kinetic hydrate inhibition efficiency than Gaffix® VC-713. This is in agreement with the observations reported by other researchers.

Tests also were conducted on 0.5 % Luvicap® EG to investigate the effect of T_e. The solution was tested at both $T_e = T_{onset} + 1.0$ ℃ and $T_e = T_{onset} - 1.0$ ℃. The results are shown in Figure 3.24. Similar to the solution containing Gaffix® VC-713, when T_e = -2.2 ℃, hydrate formation started at t_i = 400 sec and full blockage was observed when t_{end} = 1,860 sec. When T_e = -0.2 ℃, there was no hydrate blockage after 4 hours. Spike peaks of homogeneous nucleation also were observed. The results again indicate that, when the temperature of the hydrate-forming solution is lower than its T_{onset}, hydrates form rapidly regardless of the presence of the inhibitors, while, when T_e is higher than its T_{onset}, the hydrate-forming solution stays in the kinetically metastable stage for a period of time. This is demonstrated by photographs taken of the samples after testing. The photograph shown in Figure 3.25 is the hydrates blockage removed from the measuring

cylinder of the test using 0.5 % Luvicap® EG at T_e = -2.2 ℃. The photograph in Figure 3.26 shows the sample after testing 0.5 % Luvicap® EG at T_e = -0.2 ℃. A few hydrate crystals were seen in the measuring cell. No hydrates blockage was found in the measuring cylinder.

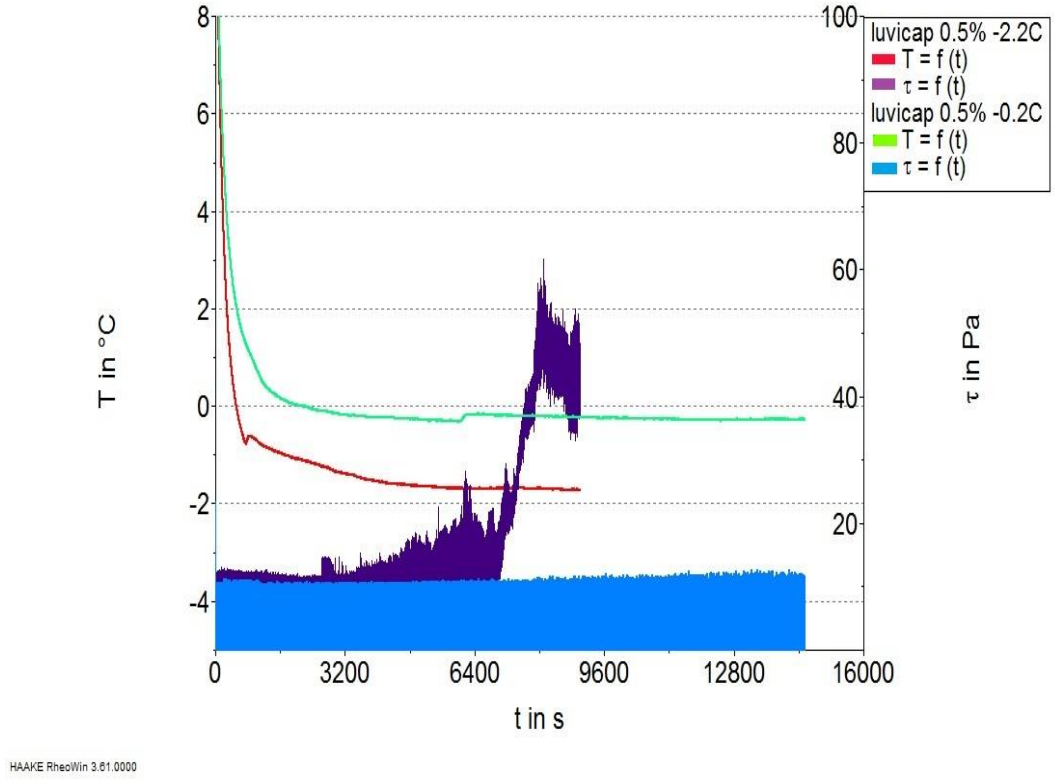

Figure 3.24 The 0.5 % Luvicap® EG hydrate-forming solution at T_e = -2.2 ℃ and T_e = -0.2 ℃

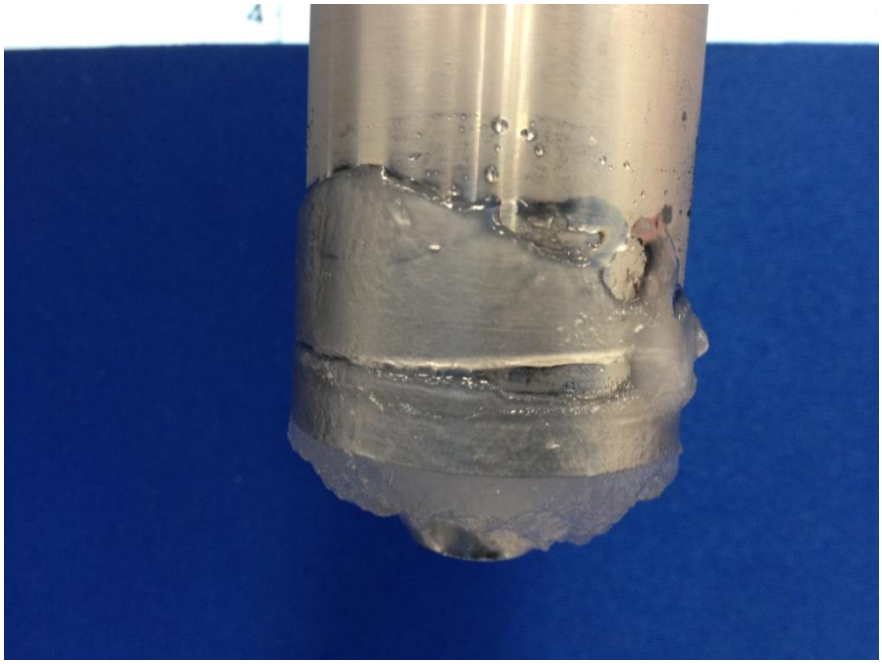

Figure 3.25 Hydrate blockage formed in 0.5 % Luvicap® EG tested at T_e = -2.2 ℃

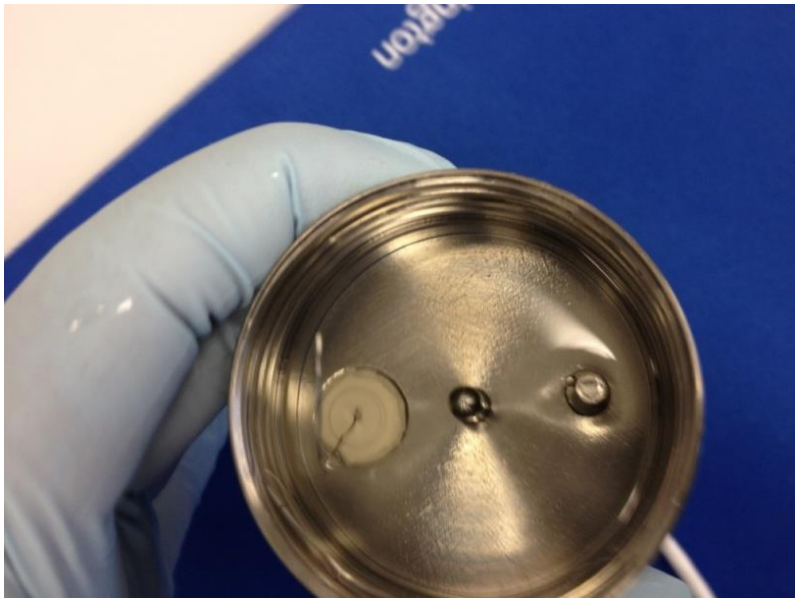

Figure 3.26 Post-testing sample of 0.5 % Luvicap® EG solution at T_e = -0.2 ℃

3.4 Conclusions

This chapter has reported the investigation of two KHIs using a rheometer. It has been demonstrated that the higher concentration of KHI appeared to lower onset temperature (T_{onset}) and increase total plugging time (t_{tp}) of the hydrate-forming solution. T_{onset} was correlated with both the type of KHI and the concentrations of KHIs. Meanwhile, the solvents of the two KHIs also played an important role in the hydrate inhibition process. Above certain levels of those solvents, 2.0 % for ethanol and 0.3 % for ethylene glycol, the solvents contributed considerable benefit to the hydrate inhibiting system as synergists.

Results of various $T_e = T_{onset}$ +/- 1.0 ℃ tests demonstrated the importance of T_{onset} in the evaluation of KHIs and their applications. Both KHIs only presented their superior kinetic hydrate performance when the T_e was above the T_{onset}. This information is valuable for the selection of KHIs and their dosage in field applications.

The results also demonstrated that the rheological measurements presented in this chapter prove a convenient and valuable method for KHI investigation. The rheological method can produce detailed information of hydrate formation and inhibition using key parameters, including t_i, T_{onset}, τ_{max} and $t_{tp.}$

It is worth mentioning that a number of rheological tests on the Gaffix®VC-713

THF hydrate-forming solution at T_e = -10 ℃ also have been conducted. The results show that there is no obvious drifting of T_{onset} from T_e = -5 ℃ to T_e = -10 ℃ at the same KHI concentration. Further investigation of the co-relationship between cooling rate and T_{onset} will require a more accurate temperature control system. This is a topic for another research thesis.

CHAPTER 4 Conclusions

From the studies reported in this thesis, the following conclusions can be drawn.

This research has demonstrated that the performance of KHIs is affected significantly by the concentration of the inhibitors, the salt strength and the presence of solvents, particularly ethanol and ethylene glycol which are used in the industry as thermodynamic gas hydrate inhibitors. The concept of SCC was proposed for each of the inhibitors used in this study. The SCC value is dependent not only on the type of KHI but also on the additives in the test solutions, such as salts and solvents. Evaluation and comparison of the inhibition performance of different KHIs should consider only the measured results at equal to or above their SCCs. Salt and solvent concentrations, and other additives present in the operating systems, must be considered when a suitable concentration is determined for the field application of the KHIs.

This work also demonstrated the importance of T_{onset} in KHI evaluation and their applications. T_{onset} was correlated with both the type of KHI and their concentrations. A higher concentration of KHI appeared to lower T_{onset} and increase total plugging time (t_{tp}) of the hydrate-forming solution. Meanwhile, the solvents in the two KHIs also played an important role in the hydrate inhibition process. Results of various $T_e = T_{onset}$ +/-1.0 ℃ tests demonstrated that KHIs only present their superior kinetic hydrate performance when the T_e is above the T_{onset}.

This information is valuable for selection of KHIs and their dosage in field applications.

The study also demonstrated that the rheological measurement approach is a convenient and reliable method for KHI investigation. In comparison with the ball-stop rig method, rheological measurement provides more details regarding the inhibition behaviour. All collectable parameters, including t_i, T_{onset}, τ_{max} and t_{tp}, are very useful in interpreting and understanding the hydrate inhibition process. It is believed that this work has produced valuable information for understanding the inhibition mechanism, allowing optimization of KHI parameters in the field and further evaluation of the chosen KHIs. Future work should be focused on the inhibition process under a controlled and slower cooling rate. Similar approaches should be employed directly for natural gas hydrate-forming solutions.

References

ALAPATI, R. & DAVIS, A. 2007. *Oil-soluble LDHI represents new breed of hydrate inhibitor* [Online]. JPT Online: Tech Up (6).

ANDERSON, B., BORGHI, G. P., TESTER, J. W. & TROUT, B. 2006. Design of natural gas hydrate inhibitors from a mechanistic understanding. *Abstracts of Papers of the American Chemical Society,* 232**,** 901-901.

ARJMANDI, M., REN, S. & TOHIDI, B. 2003. Progress in Design and Asessment of Low Dosage Hydrate Inhibitors. *Offshore Mediterranean Conference*. Ravenna, Italy.

BEAUCHAMP, B. 2004. Natural gas hydrates: myths, facts and issues. *Comptes Rendus Geoscience,* 336**,** 751-765.

BISHNOI, P. R. & DHOLABHAI, P. D. 1999. Equilibrium conditions for hydrate formation for a ternary mixture of methane, propane and carbon dioxide, and a natural gas mixture in the presence of electrolytes and methanol. *Fluid Phase Equilibria,* 158**,** 821-827.

BOBEV, S. & TAIT, K. T. 2004. Methanol - inhibitor or promoter of the formation of gas hydrates from deuterated ice? *American Mineralogist,* 89**,** 1208-1214.

CHATTI, I., DELAHAYE, A., FOURNAISON, L. & PETITET, J. P. 2005. Benefits and drawbacks of clathrate hydrates: a review of their areas of interest. *Energy Conversion and Management,* 46**,** 1333-1343.

CHUA, P. C., SÆBØ, M., LUNDE, L. & KELLAND, M. A. 2011. Dual Kinetic Hydrate Inhibition and Scale Inhibition by Polyaspartamides. *Energy & Fuels,* 25**,** 5165-5172.

CHUN, M. K., LEE, H. & RYU, B. J. 2000. Phase equilibria of R22 (CHClF2) hydrate systems in the presence of NaCl, KCl, and $MgCl_2$. *Journal of Chemical and Engineering Data,* 45**,** 1150-1153.

CLAIRE, R. 2006. *Interpreting Thermal Analysis Data* [Online]. MMS Conferencing. Available: www.mmsconferencing.com/pdf/eyp/c.rawlinson.pdf [Accessed 15/09/2012 2012].

CLEGG, D. W. & COLLYER, A. A. 1998. *Rheological measurement,* London, Chapman & Hall.

CONG, Y., ZHAO, S. & HUANG, W. 2011. Study on Flame-Retardant Asphalt with Storage Stability. *Petroleum Science and Technology,* 29**,** 1197-1201.

DAVENPORT, J. R., MUSA, O. M., PATERSON, M. J., PIEPENBROCK, M. O. M., FUCKE, K. & STEED, J. W. 2011. A simple chemical model for clathrate hydrate inhibition by polyvinylcaprolactam. *Chemical Communications,* 47**,** 9891-9893.

DAWE, R. A. & THOMAS, S. 2007. A large potential methane source - Natural gas hydrates. *Energy Sources Part A - Recovery Utilization and Environmental Effects,* 29**,** 217-229.

DEL VILLANO, L. & KELLAND, M. A. 2011. An investigation into the laboratory method for the evaluation of the performance of kinetic hydrate inhibitors using superheated gas hydrates. *Chemical Engineering Science,* Vol.66**,** 1973-1985

DEL VILLANO, L., KOMMEDAL, R. & KELLAND, M. A. 2008. Class of kinetic hydrate inhibitors with good biodegradability. *Energy & Fuels,* 22**,** 3143-3149.

DELAHAYE, A., FOURNAISON, L., JERBI, S. & MAYOUFI, N. 2011. Rheological Properties of CO_2 Hydrate Slurry Flow in the Presence of Additives. *Industrial & Engineering Chemistry Research,* 50**,** 8344-8353.

DHOLABHAI, P. D., KALOGERAKIS, N. & BISHNOI, P. R. 1993. Kinetics of Methane Hydrate Formation in Aqueous-Electrolyte Solutions. *Canadian Journal of Chemical Engineering,* 71**,** 68-74.

DHOLABHAI, P. D., PARENT, J. S. & BISHNOI, P. R. 1997. Equilibrium conditions for hydrate formation from binary mixtures of methane and carbon dioxide in the presence of electrolytes, methanol and ethylene glycol. *Fluid Phase Equilibria,* 141**,** 235-246.

ENGLEZOS, P. 1993. Clathrate Hydrates. *Industrial & Engineering Chemistry Research,* 32**,** 1251-1274.

ENGLEZOS, P. & LEE, J. D. 2005. Gas hydrates: A cleaner source of energy and opportunity for innovative technologies. *Korean Journal of Chemical Engineering,* 22**,** 671-681.

FIDEL-DUFOUR, A., GRUY, F. & HERRI, J. M. 2006. Rheology of methane hydrate slurries during their crystallization in a water in dodecane emulsion under flowing. *Chemical Engineering Science,* 61**,** 505-515.

FOURNAISON, L., DELAHAYE, A., CHATTI, I. & PETITET, J. P. 2004. CO_2 hydrates in refrigeration processes. *Industrial & Engineering Chemistry Research,* 43**,** 6521-6526.

FREER, E. M. & SLOAN, E. D. 2000. An engineering approach to kinetic inhibitor design using molecular dynamics simulations. *Gas Hydrates: Challenges for the Future,* 912**,** 651-657.

GAILLARD, C., MONFORT, J. P. & PEYTAVY, J. L. 1999. Investigation of methane hydrate formation in a recirculating flow loop: Modeling of the kinetics and tests of efficiency of chemical additives on hydrate inhibition. *Oil & Gas Science and Technology-Revue De L Institut Francais Du Petrole,* 54**,** 365-374.

HALD, K. & NULAND, S. 2007. Hydrate slurry rheology in the petroleum industy. *ANNUAL TRANSACTIONS OF THE NORDIC RHEOLOGY SOCIETY,* 15.

HALVORSEN, V. H., LERVIK, J. K. & KLEVJER, G. 2000. Hydrate and wax prevention of risers by electrical heating. *Proceedings of the 10th (2000) International Offshore and Polar Engineering Conference, Vol II***,** 42-48.

HAMMERSCHMIDT, E. G. 1934. Formation of gas hydrates in natural gas transmission lines. *Ind. Eng. Chem,* 26**,** 851-855.

HAWTIN, R. W. & RODGER, P. M. 2006. Polydispersity in oligomeric low dosage gas hydrate inhibitors. *Journal of Materials Chemistry,* 16**,** 1934-1942.

HEIDARYAN, E., SALARABADI, A., MOGHADASI, J. & DOURBASH, A. 2010. A new high performance gas hydrate inhibitor. *Journal of Natural Gas Chemistry,* 19**,** 323-326.

HUO, Z., FREER, E., LAMAR, M., SANNIGRAHI, B., KNAUSS, D. M. & SLOAN, E. D. 2001. Hydrate plug prevention by anti-agglomeration. *Chemical Engineering Science,* 56**,** 4979-4991.

JAGER, M. D., BALLARD, A. L. & SLOAN, E. D. 2005. Comparison between experimental data and aqueous-phase fugacity model for hydrate prediction. *Fluid Phase Equilibria,* 232**,** 25-36.

KELLAND, M. A. 2006. History of the development of low dosage hydrate inhibitors. *Energy & Fuels,* 20**,** 825-847.

KELLAND, M. A., KVÆSTAD, A. H. & ASTAD, E. L. 2012. Tetrahydrofuran Hydrate Crystal Growth Inhibition by Trialkylamine Oxides and Synergism with the Gas Kinetic Hydrate Inhibitor Poly(N-vinyl caprolactam). *Energy & Fuels,* 26**,** 4454-4464.

KELLAND, M. A., MONIG, K., IVERSEN, J. E. & LEKVAM, K. 2008. Feasibility study for the use of kinetic hydrate inhibitors in deep-water drilling fluids. *Energy & Fuels,* 22**,** 2405-2410.

KELLAND, M. A., SVARTAAS, T. M., OVSTHUS, J. & NAMBA, T. 2000. A new class of kinetic hydrate inhibitor. *Gas Hydrates: Challenges for the Future,* 912**,** 281-293.

KELLAND, M. A., SVARTAS, T. M. & ANDERSEN, L. D. 2009. Gas hydrate anti-agglomerant properties of polypropoxylates and some other demulsifiers. *Journal of Petroleum Science and Engineering,* 64**,** 1-10.

KERR, R. A. 2004. Energy - Gas hydrate resource: Smaller but sooner. *Science,* 303**,** 946-947.

KNEPPER, S., WIENEKE, M. & MORRISSEY, C. 2009. Subsea Control Fluids. Avoidance of Hydrate Formation. *Measurement & Control,* 42**,** 140-144.

KOH, C. A. 2002. Towards a fundamental understanding of natural gas hydrates. *Chemical Society Reviews,* 31**,** 157-167.

KVENVOLDEN, K. A. 1988. Methane Hydrate - a Major Reservoir of Carbon in the Shallow Geosphere. *Chemical Geology,* 71**,** 41-51.

LACHANCE, J. W., SLOAN, E. D. & KOH, C. A. 2009. Determining gas hydrate kinetic inhibitor effectiveness using emulsions. *Chemical Engineering Science,* 64**,** 180-184.

LEDERHOS, J. P., LONG, J. P., SUM, A., CHRISTIANSEN, R. L. & SLOAN, E. D. 1996. Effective kinetic inhibitors for natural gas hydrates. *Chemical Engineering Science,* 51**,** 1221-1229.

LIU, M. F., ZHANG, X., ZAMMARANO, M., GILMAN, J. W. & KASHIWAGI, T. 2011. Flame retardancy of poly(styrene-co-acrylonitrile) by the synergistic interaction between clay and phosphomolybdate hydrates. *Polymer Degradation and Stability,* 96**,** 1000-1008.

LONG, J. P., LEDERHOS, J. P., SUM, A., CHRISTIANSEN, R. L. & SLOAN, E. D. Kinetic inhibitors of natural gas hydates. 73rd Gas Processors Association Annual Convention 7-9 March 1994 New Orlwans, LA. 85-93.

LONG, J. P. & SLOAN, E. D. 1993. Quantized Water Clusters around Apolar Molecules. *Molecular Simulation,* 11**,** 145-161.

LOU, X., DING, A. L., MAEDA, N., WANG, S., KOZIELSKI, K. & HARTLEY, P. G. 2012. Synthesis of Effective Kinetic Inhibitors for Natural Gas Hydrates *Energy & Fuels,* 26**,** 1037-1043.

LOVEDAY, J. S., NELMES, R. J., GUTHRIE, M., BELMONTE, S. A., ALLAN, D. R., KLUG, D. D., TSE, J. S. & HANDA, Y. P. 2001. Stable methane hydrate above 2 GPa and the source of Titan's atmospheric methane. *Nature,* 410**,** 661-663.

MACOSKO, C. W. 1994. *Rheology - Principles, Measurements and Applications*, John Wiley & Sons.

MAHAJAN, D., TAYLOR, C. E. & MANSOORI, G. A. 2007. An introduction to natural gas hydrate/clathrate: The major organic carbon reserve of the Earth. *Journal of Petroleum Science and Engineering,* 56**,** 1-8.

MAKOGON, I. F. 1997. *Hydrates of hydrocarbons*, Tulsa, Oklahoma., Penn Well Publishing Company.

MAKOGON, T. Y., LARSEN, R., KNIGHT, C. A. & SLOAN, E. D. 1997. Melt growth of tetrahydrofuran clathrate hydrate and its inhibition: method and first results. *Journal of Crystal Growth,* 179**,** 258-262.

MAKOGON, Y. F., HOLDITCH, S. A. & MAKOGON, T. Y. 2007. Natural gas-hydrates - A potential energy source for the 21st Century. *Journal of Petroleum Science and Engineering,* 56**,** 14-31.

MAKOGON, Y. F., MAKOGON, T. Y. & HOLDITCH, S. A. 2000. Kinetics and mechanisms of gas hydrate formation and dissociation with inhibitors. *Gas Hydrates: Challenges for the Future,* 912**,** 777-796.

MALKIN, A. Y. & ISAYEV, A. I. 2006. *Rheology: concepts, methods & applicaitons* Tornoto, ChemTec Publishing.

MEHTA, A. P. & SLOAN, E. D. 1996. Improved thermodynamic parameters for prediction of Structure H hydrate equilibria. *Aiche Journal,* 42**,** 2036-2046.

MOKHATAB, S., WILKENS, R. J. & LEONTARITIS, K. J. 2007. A review of strategies for solving gas-hydrate problems in subsea pipelines. *Energy Sources Part A - Recovery Utilization and Environmental Effects,* 29**,** 39-45.

MORIDIS, G. J., REAGAN, M. T., BOYLE, K. L. & ZHANG, K. N. 2011. Evaluation of the Gas Production Potential of Some Particularly Challenging Types of Oceanic Hydrate Deposits. *Transport in Porous Media,* 90**,** 269-299.

MORRISON, F. A. 2001. *Understanding rheology* New York, Oxford University Press.

NG, H. J. & ROBINSON, D. B. 1985. Hydrate Formation in Systems Containing Methane, Ethane, Propane, Carbon-Dioxide or Hydrogen-Sulfide in the Presence of Methanol. *Fluid Phase Equilibria,* 21**,** 145-155.

O'REILLY, R., IEONG, N. S., CHUA, P. C. & KELLAND, M. A. 2011. Missing Poly(N -vinyl lactam) Kinetic Hydrate Inhibitor: High-Pressure Kinetic Hydrate Inhibition of Structure II Gas Hydrates with Poly(N -vinyl piperidone) and Other Poly(N -vinyl lactam) Homopolymers. *Energy & Fuels,* 25**,** 4595-4599.

OGAWA, T., ITO, T., WATANABE, K., TAHARA, K. I., HIRAOKA, R., OCHIAI, J. I., OHMURA, R. & MORI, Y. H. 2006. Development of a novel hydrate-based refrigeration system: A preliminary overview. *Applied Thermal Engineering,* 26**,** 2157-2167.

PEIXINHO, J., KARANJKAR, P. U., LEE, J. W. & MORRIS, J. F. 2010. Rheology of Hydrate Forming Emulsions. *Langmuir,* 26**,** 11699-11704.

PICKERING, P. F., EDMONDS, B., MOORWOOD, R. A. S., SZCZEPANSKI, R. & WATSON, M. J. 2001. Evaluating new chemicals and alternatives for mitigating hyrates in Oil and Gas production. *IIR Conference*. Aberdeen, Scotland.

PURWANTO, Y. A., OSHITA, S., SEO, Y. & KAWAGOE, Y. 2001. Concentration of liquid foods by the use of gas hydrate. *Journal of Food Engineering,* 47**,** 133-138.

RENSING, P. J., LIBERATORE, M. W., KOH, C. A. & SLOAN, E. D. 2008. Rheological Investigation of Hydrate Slurries. *The 6th International Conference on Gas Hydrates.* Vancouver, British Columbia, CANADA.

RENSING, P. J., LIBERATORE, M. W., SUM, A. K., KOH, C. A. & SLOAN, E. D. 2011. Viscosity and yield stresses of ice slurries formed in water-in-oil emulsions. *Journal of Non-Newtonian Fluid Mechanics,* 166**,** 859-866.

RIBEIRO, C. P. & LAGE, P. L. C. 2008. Modelling of hydrate formation kinetics: State-of-the-art and future directions. *Chemical Engineering Science,* 63**,** 2007-2034.

RIPMEESTER, J. A., TSE, J. S., RATCLIFFE, C. I. & POWELL, B. M. 1987. A New Clathrate Hydrate Structure. *Nature,* 325**,** 135-136.

ROJAS, Y. V., PHAN, C. M. & LOU, X. 2010. Dynamic surface tension studies on poly(N-vinylcaprolactam/N-vinylpyrrolidone/N,N-dimethylaminoethyl methacrylate) at the air-liquid interface. *Colloids and Surfaces a-Physicochemical and Engineering Aspects,* 355**,** 99-103.

SCHULLER, R. B., TANDE, M. & KVANDAL, H. K. 2005. Rheological hydrate detection and characterization. *ANNUAL TRANSACTIONS OF THE NORDIC RHEOLOGY SOCIETY,,* 13**,** 83-90.

SEFIDROODI, H., CHUA, P. C. & KELLAND, M. A. 2011. THF hydrate crystal growth inhibition with small anionic organic compounds and their synergistic properties with the kinetic hydrate inhibitor poly(N-vinylcaprolactam). *Chemical Engineering Science,* 66**,** 2050-2056.

SHERMAN, L. M. 2004. *Rheometers: Which Type Is Right for You?* [Online]. PlasticsTechnology Available: http://www.ptonline.com/articles/rheometers-which-type-is-right-for-you [Accessed 18 January 2012].

SLOAN, E. D. 1998a. *Clathrate Hydrates of Natural Gases,* New York, Marcel Dekker Inc.

SLOAN, E. D. 1998b. Gas hydrates: Review of physical/chemical properties. *Energy & Fuels,* 12**,** 191-196.

SLOAN, E. D. 2003a. Clathrate hydrate measurements: microscopic, mesoscopic, and macroscopic. *Journal of Chemical Thermodynamics,* 35**,** 41-53.

SLOAN, E. D. 2003b. Fundamental principles and applications of natural gas hydrates. *Nature,* 426**,** 353-359.

SLOAN, E. D. & FLEYFEL, F. 1992. Hydrate Dissociation Enthalpy and Guest Size. *Fluid Phase Equilibria,* 76**,** 123-140.

SLOAN, E. D. & KOH, C. A. 2008. *Clathrate hydrates of natural gases,* Boca Raton, Florida Taylor & Francis Group.

SLOAN, E. D., SUBRAMANIAN, S., MATTHEWS, P. N., LEDERHOS, J. P. & KHOKHAR, A. A. 1998. Quantifying hydrate formation and kinetic inhibition. *Industrial & Engineering Chemistry Research,* 37**,** 3124-3132.

TALAGHAT, M. R., ESMAEILZADEH, F. & FATHIKALJAHI, J. 2009. Experimental and theoretical investigation of simple gas hydrate formation with or without presence of kinetic inhibitors in a flow mini-loop apparatus *Fluid Phase Equilibria,* Vol.279**,** 28-40.

URDAHL, O., LUND, A., MORK, P. & NILSEN, T. N. 1995a. Inhibition of Gas Hydrate Formation by Means of Chemical Additives .1. Development of an Experimental Set-up for Characterization of Gas Hydrate Inhibitor Efficiency with Respect to Flow Properties and Deposition. *Chemical Engineering Science,* 50**,** 863-870.

WANG, L. K., CHEN, G. J., HAN, G. H., GUO, X. Q. & GUO, T. M. 2003. Experimental study on the solubility of natural gas components in water with or without hydrate inhibitor. *Fluid Phase Equilibria,* 207**,** 143-154.

WU, H.-J. & ENGLEZOS, P. 2006. Inhibiting Effect of Triethylene Glycol and Glycerol on Gas Hydrate Formation Conditions. *Journal of Chemical & Engineering Data,* 51**,** 1811-1813.

WU, M., WANG, S. & LIU, H. 2007. A study on inhibitors for the prevention of hydrate formation in gas transmission pipeline. *Journal of Natural Gas Chemistry,* 16**,** 81-85.

XIE, Y. M., GUO, K. H., LIANG, D. Q., FAN, S. S. & GU, J. M. 2005. Steady gas hydrate growth along vertical heat transfer tube without stirring. *Chemical Engineering Science,* 60**,** 777-786.

XIE, Y. M., LI, G., LIU, D. P., LIU, N., QI, Y. X., LIANG, D. Q., GUO, K. H. & FAN, S. S. 2010. Experimental study on a small scale of gas hydrate cold storage apparatus. *Applied Energy,* 87**,** 3340-3346.

YOUSIF, M. H. 1998. Effect of underinhibition with methanol and ethylene glycol on the hydrate-control process. *SPE Production & Facilities,* 13**,** 184-189.

YOUSIF, M. H., DORSHOW, R. B. & YOUNG, D. B. 1994. Testing of Hydrate Kinetic Inhibitors Using Laser-Light Scattering Technique. *International Conference on Natural Gas Hydrates,* 715**,** 330-340.

YOUSIF, M. H. & YOUNG, D. B. 1994. A Simple Thermodynamic Model to Predict the Hydrate Temperature Suppression in Aqueous Solutions of Salts and Alcohols. *Seventy-Third Annual Convention - Gas Processors Association, Proceedings***,** 94-99.

YU, D. & CHENG, X. J. 2009. Research into Problems of Plugged Submarine Gas Line in the Bo-Xi Oil Field. *IPC2008: Proceedings of the Asme International Pipeline Conference - 2008, Vol 1***,** 77-81.

ZENG, H., MOUDRAKOVSKI, I. L., RIPMEESTER, J. A. & WALKER, V. K. 2006. Effect of antifreeze protein on nucleation, growth and memory of gas hydrates. *Aiche Journal,* 52**,** 3304-3309.

ZHANG, Y. F., DEBENEDETTI, P. G., PRUD'HOMME, R. K. & PETHICA, B. A. 2004. Differential scanning calorimetry studies of clathrate hydrate formation. *Journal of Physical Chemistry B,* 108**,** 16717-16722.